

上海交通大学

SHANGHAI JIAO TONG UNIVERSITY

学士学位论文

BACHELOR' S THESIS



论文题目：面向胃肠道无创诊查的微型仿生
机器人无线通信系统研究

学生姓名：_____王艺芸_____

学生学号：_____515030910129_____

专 业：_____测控技术与仪器_____

指导教师：_____颜国正_____

学院(系)：电子信息与电气工程学院

Bachelor Thesis in Instrument Science and Engineering

Research on Wireless Communication System of Micro Bionic Robot for Noninvasive Gastrointestinal Diagnosis

Yiyun Wang

Advisor

Prof. Guozheng Yan

Department of Instrument Science and Engineering

School of Electronic Information and Electrical Engineering

Shanghai Jiao Tong University

Shanghai, P.R.China

面向胃肠道无创诊查的微型仿生机器人无线通信系统研究

摘要

胃肠道疾病是临床上的常见病。传统的胃镜、肠镜总是在诊疗时给患者带来痛苦并造成各种并发症。现有的胶囊内镜因多为被动式工作，且存在供能不足的问题，而使其应用受限。因此，主动式面向胃肠道无创诊察的无线供能微型仿生机器人的研发日益得到重视。为满足机器人系统从上位机到机器人端的通信需求，实现有效、稳定的运动控制，无线通信系统的研究尤为关键。

本文首先调查了国内外胶囊机器人研究现状，分析总结了不同无线通信技术的优缺点及不同应用场景下无线通讯系统的设计方案。

随后，建立了无线通讯模块的总体结构，设计并制作了体内外无线通信子模块的软硬件系统。通过对无线通信系统的组装及联调，实现了直流供电情况下的稳定通信及机器人控制。同时，设计了人机交互界面以更加直观、便捷地使用计算机控制机器人的运动。

在此基础上，针对无线供能情况下所遇到的通信不稳定问题，整合机械子系统、无线供能子系统、照明子系统，从能量发射、能量管理、能量传输效率、通讯逻辑四方面进行实验优化并解决了机器人通信不稳定的问题。通过完善机器人通信系统逻辑并结合实验论证，实现了无线供能情况下机器人的可靠通信。

最后，对研究结果进行了分析与总结，对机器人系统中仍存在的其他问题提出未来解决方案。

关键词：胃肠道无创诊察，微型仿生机器人，无线通信系统，软硬件设计

Research on Wireless Communication System of Micro Bionic Robot for Noninvasive Gastrointestinal Diagnosis

ABSTRACT

Gastrointestinal diseases are common clinical diseases. Traditional endoscopes always bring enormous pain along with series of complications. Free from current endoscopes' limitations such as insufficient power supply and passive movement, active micro bionic robots for noninvasive gastrointestinal diagnosis with wireless power supply gain increasing attention. This study satisfies the communication requirement of the robot system from the host computer to the robot and realizes the effective and stable control, therefore, it is of great importance.

This paper firstly reviews on current progresses and achievements of the micro gastrointestinal bionic robot from domestics and overseas. Next, the advantages and disadvantages of different wireless communication technology are included and the schemes of wireless communication system are designed and analyzed. Then, the overall structure design of the wireless communication module, the internal and external PCB boards, and programming schemes on the Microcontroller Unit (MCU) are introduced. Through assembly and debugging of the wireless communication module, the communication and robot control under direct current (DC) power supply is stable. Moreover, an integrated interactive interface fulfills robot movement control in a direct and convenient way.

Focusing on the unstable communication under wireless power supply with other modules attached, experiments are designed and carried out from four aspects, namely the power transmitter, the power management circuit, the transmission efficiency and power consumption. Besides, through optimizing the system logic and

demonstrating experiment, this study realizes the reliable communication under wireless power supply.

At last, the paper analyzes the results and gives an overall conclusion, together with future works in concern of other existing problems.

Key words: Noninvasive gastrointestinal diagnosis, Micro bionic robot, Wireless Communication System, Software and hardware design

Contents

Chapter One	Introduction	1
1.1	Research Background and Significance	1
1.2	Development of Micro Gastrointestinal Bionic Robot Technology	3
1.2.1	Traditional Endoscopes	3
1.2.2	Capsule Endoscopes	5
1.3	Brief Introduction of Wireless Communication System	9
1.4	Reviews on Wireless Communication System	11
1.5	Objectives and Methodology	14
Chapter Two	Hardware Design of the Wireless Communication System	16
2.1	Design of the External Wireless Communication Module	17
2.2	Design of the Internal Wireless Communication Module	21
Chapter Three	Software Design of the Wireless Communication System	30
3.1	Programming of the External Communication Module	30
3.2	Programming of the Internal Communication Module	34
3.3	Hardware and Software Debugging	38
3.4	Programming of the Integrated Interactive Interface	39
Chapter Four	Experimental Verification and Result Analysis	43
4.1	Transmitting Side Reconstruction	46
4.2	Energy Management Circuit	47
4.3	Multi-coil Wireless Power Transmission	49
4.4	Voltage Regulator Chip Reselection	52
4.5	Programming Optimization	54
Chapter Five	Conclusions and Future Works	64
5.1	Conclusions	64
5.2	Future Works	65
REFERENCE	68
ACHIEVEMENTS DURING THE STUDY FOR BACHELOR'S DEGREE	70
ACKNOWLEDGEMENTS	71

Chapter One Introduction

Micro bionic robot providing noninvasive gastrointestinal diagnosis with high efficiency and convenience has become the research focus in the field of endoscopy technology. With the rapid development of Micro-Electro-Mechanical System (MEMS) and the urgent demand of the market, more requirements have been put towards micro bionic robots. This chapter briefly introduces the research background and significance at first. Then, the technology development is recorded, followed by a brief introduction of the wireless communication system. At last, main content of this paper is reported.

1.1 Research Background and Significance

Gastrointestinal diseases have long been common clinical diseases, including ulcers, gastrointestinal malignancies, gastroenteritis and Crohn's diseases, which seriously endanger health. In recent years, due to the rapid pace of modern life, high work pressure, environmental pollution, irregular diet and food safety problems, an increasing number of people are under sub-health state and suffer from various gastrointestinal diseases mentioned above. The morbidity and mortality have kept an upward trend. As the data established by the World Health Organization, in 2018, an estimated 18.1 million people would be diagnosed with cancer and about 9.6 million people would die of cancer. The rank of new cancers incidence worldwide were lung cancer (11.6%), breast cancer (11.6%), colorectal cancer (10.2%), prostate cancer (7.1%) and gastric cancer (5.7%).^[1] In other words, gastrointestinal cancer takes the lead in cancer incidence. It has become a major disease, endangering people all over

the world and a public health issue which needs urge movement. A case-control study and a cohort study in Japan reported a 30–65% reduction in gastric cancer mortality when screening was undertaken via endoscopy.^[2] The researchers in China also noted that the 5-year survival rate after radical resection of early colorectal could reach over 90%, while the survival rate of advanced colorectal cancer was only 7%. The complete resection rate of early colorectal cancer under endoscopy was over 80%, and the recurrence rate in situ was meager.^[3] Therefore, early diagnosis and treatment of gastrointestinal cancer plays a vital role in saving the lives of cancer patients.

A big obstacle stands in the way of early diagnosis and treatment of gastrointestinal cancer is the predicament of diagnosis. Nowadays, clinical still uses traditional fiber-optic endoscope to make early diagnosis operations for patients. Most commonly used method of applying fiber-optic endoscope in practice is inserting the instrument from the mouth or anus into body for detection which causes great discomfort. Despite the agonizing feelings during the examination, common complications like perforation, hemorrhage, and respiratory problems along with less severe complications such as cardiac alterations, transient bacteriemia all brings patients unutterable pains.^[4] Numerous researches had studied the complications and hazards of gastrointestinal endoscopy. With flexible instruments, perforations caused by exertion of force in attempting to pass the endoscope further through the cricopharynx usually took place in the hypopharynx or cervical esophagus.^[5] The size of the endoscope sometimes leads to respiratory. Thus, people tend to avoid endoscopy, which is an effective way for early diagnosis and hold up the best moment for diagnostic time and treatment. Nowadays, there have been certain succedaneums for traditional endoscopy, such as fecal occult blood test, serological tumor marker detection and barium enema, but their diagnostic effect is not so ideal.^[6] Besides, because of the complex internal structure of the human body, especially the narrow and tortuous digestive tract, in some circumstances, certain specific locations can hardly be detected. In 2000, the first capsule endoscope got the approval of the Food and Drug Administration (FDA) to be applied in clinic. However, up until now, the

capsule endoscopes still take passive movement, that is, progressing with the natural peristalsis of the digestive tract. For digestive organs as large as the stomach, due to the limited scope of observation, there will be a considerable omission diagnosis. Moreover, they have shortcomings like missed diagnosis, being incapable of fixed-point diagnosis and long-term diagnosis. As a result, capsule endoscopes have not been widely promoted.

1.2 Development of Micro Gastrointestinal Bionic Robot Technology

1.2.1 Traditional Endoscopes

Today, digestive endoscope has become a relatively common medical device. Its main working method is to enter human body through natural channels to observe lesions in relevant parts and carry out treatment. Compared with China, the gastrointestinal endoscope has enjoyed a history of more than 200 years in the development of Western medicine since in 1806 when a German doctor first proposed the idea. Generally speaking, the development of endoscope has gone through three stages. First stage (1795-1932) is the era of hard tube ones. Second stage (1932-1980) belongs to fiber endoscope which was later equipped with ultrasonic function. The third stage (since 1980) witnessed the development of the electronic ones.^[7]

In 1970s, our country imported fiber-optic ones. In 1983, American company Welch Allyn first established electronic video endoscope. After that, some research instituted in Western Europe and Japan made various investigations on the electronic endoscope. In 1985, our country imported ultrasonic endoscopes from Olympus and made clinical application report in 1987.^[8] Electronic ones were widely promoted throughout our country in 1990s. Nowadays, the market all over the world was merely monopolized by Japanese company Olympus.^[9] With the unremitting efforts of outstanding professors, the diagnostic level of digestive system diseases in China has

significantly improved. Diagnostic tools such as gastro scope, colonoscope, double-balloon endoscope, choledochoscope, magnifying endoscope, ultrasonic endoscope and electronic staining endoscope are all available. Meanwhile, in clinical of small bowel, endoscopes include single-balloon and double-balloon electronic ones. Double-balloon endoscopies have been widely applied since 2003 worldwide while single-balloon ones have been applied since 2007. In 2009, spiral endoscope came onto the stage.

Table 1.1 shows the characteristics of the endoscopes in different stages.

Table 1.1 Comparison of Main Performance of Wireless Communication

Type	Period	Deficiencies	Main applications
Hard tube endoscopes	1795-1932	Difficult to operate, blurred imaging, many blind spots, risk of burns	Rectum, urinary system, stomach
Fiber endoscopes	1932-1980	Flexibility, fewer blind spots, discomforts	Digestive system, urinary system
Electronic endoscopes	since 1980	High resolution, smaller size, recording ability, discomforts	Digestive system, urinary system

At present, the most commonly used and effective tool is the electronic video endoscope. By inserting a slender flexible tube with a miniature camera at the front into the human body, such kind of endoscope realizes direct observation towards the lining of the intestinal tract. With specific micro-devices, such as biopsy forceps, injection needles, hemostatic clips, the endoscope can achieve biopsy and therapeutic functions as well. The imaging is clear and can be magnified. Therefore, it has a high resolution which allows it to observe the fine structure of intestinal mucosa, figure out micro-lesions to realize early detection, diagnosis and treatment.

1.2.2 Capsule Endoscopes

However, as mentioned above, traditional endoscopes all bring wretched feelings as well as complications. With the rapid development of microelectronics technology, Micro-Electro-Mechanical System, image processing technology and wireless communication technology, the aim of design a robot small in size and low in power is made possible. The research and development of capsule robots inaugurated from then on. The capsule endoscope is a small, disposable, wireless, miniature camera which permits us to get a direct visualization of the gastrointestinal mucosa.^[10]

In 2000, Israeli company Given Imaging manufactured the initial capsule endoscope named mouth to anus (M2A) initially, and PillCam Small Bowel (PillCam SB) later.^[11] The capsule contained light emitting diodes, a color camera, a lens, an antenna, two batteries and a radio frequency transmitter. The camera took two images every second and transmitted them through radio frequency to a sensor array in a belt placed around patient's abdomen and from there to a recording device in the belt. Once the process was finished, the images were downloaded to a computer workstation with the software to display images on the monitor.^[12] In 2009, PillCam series was updated to PillCam Colon 2 with two cameras and changeable video capture frequency ranging from 4 to 35 frames per second. With such improvement, it could cover a wider diagnose range and saved more power.^[13] In 2013, PillCam SB III was released, whose details were given in Table 1.2.^[14]

Later on, the colonic capsules and esophageal were launched into the market, and the patency capsule was introduced. Additional small bowel capsule systems included the Olympus EndoCapsule, the American CapsoCam SV-1, the Korean Miro pill, and the Chinese OMOM pill. The PillCam SB1, the Korean Miro Capsule and the Olympus EndoCapsule did not show much differences in comparisons. The EndoCapsule was a video capsule endoscope equipped with a charge-coupled device sensor taking place of a CMOS to acquire images. In 2005, it got launched in Europe






and in 2007, it obtained FDA clearance. Camera, light source, transmitter and batteries consisted the whole capsule. Similarly, it transmitted images to a receiver and the physician then download all images for diagnosis from the receiver.^[11]

Comparing with other similar products, the duplex multi-channel communication mode of OMOM capsule endoscope system has largely improved the controllability and convenience in clinical application. Since 2004, the company has invented various new products for different clinical uses, such as controllable ones, storable ones. The capsule could continuously capture images of the gastrointestinal tract during its movement and transmitted real-time image data wirelessly to the recorder. OMOM system had unique multichannel mode and wireless USB monitoring which meant it could undertake as many patients as the channel number simultaneously at the same location without interference. What's more, the storable capsule endoscope used a large capacity storage module instead of traditional data transmission module to store images within the internal memory module. By doing this, patients did not need to wear the recorder any more.^[11]

All these capsule endoscopes above applied the same transmission system, radio frequency. Such system made wireless endoscopes possible, however, at a high energy consuming cost, which limited the operation time and complete examination. MiRo capsule endoscope which was introduced in Korea in 2007 and was the prototype of MiroCam, used new transmission system and human body communication so as to extend the longest operation time to eleven hours. It solved the inferior image quality problem inevitably caused by data compression for efficient data transmission by using CMOS image sensor. The current required for fan-out between chips was reduced as well. ^[11]

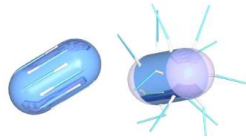
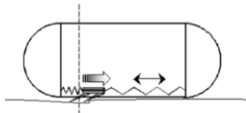

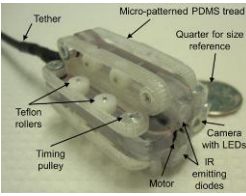
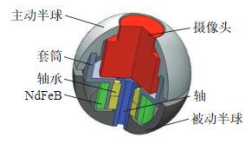

Table 1.2 is listed to present clearly the characteristic of typical passive capsule endoscopes.

Table 1.2 Characteristic of Typical Passive Capsule Endoscopes

	OMOM	EndoCapsule	MiRoCam	PillCam SB3	CaspsoCam Plus
Photo					
Diameter	11 mm	11 mm	11.6 mm	11.4 mm	11 mm
Length	25.4 mm	26 mm	24 mm	26.2 mm	31 mm
Weight	6 g	3.8 g	3.4 g	3.0 g	4.0 g
Frame /second	0.5-2	2	3/6	2-6	5×4
View range	150°	160°	170°	156°	360°
Camera position	One end	One end	Two ends	One end	Four sides
Working hour	12	12	12	8	15
FDA approval	No	Yes	No	Yes	Yes

The passive movement of capsule endoscopes entirely depends on the natural peristalsis. It leads to long diagnosis time and hinder accurate diagnosis. Therefore, techniques for active control are now developing. Magnetic steering mechanism like MiroCam Navi and internal locomotive devices like paddling-based ones has been developed. In 2004, Menciassi proposed an 8-legged capsule and Korea proposed the first inchworm-like one. In 2006, a paddling-based mechanism was invented and latter got enhanced in 2010. In 2010, a team from Singapore proposed two actuation mechanisms to increase maneuverability of the camera. Both were driven by Ion electrochemical batteries.

Table 1.3 Characteristic of Typical Passive Capsule Endoscopes

Main author	Year	Actuation mode	Photo	Speed(cm/min)
Menciassi	2004	8-legged		N/A
Kim	2004	Inchworm		1.47
Kim	2010	Paddling-based		17
Sliker	2012	Treads		18
Yongshun Zhang	2018	Universal rotating magnetic Control		N/A
Ankon	2019	Moving Magnetic control		N/A

One was based on one degree of freedom actuation and the camera could be rotated for 360° view at the cost of high energy consumption. The other could rotate the camera in two directions which had no need to be operated continuously.^[15] Sliker's team invented a tethered one in 2012.^[16] Approved in 2013, Ankon MCE System mitigated the problem that handheld generated magnetic force was insufficient. In 2015, Korean scholars established a novel electromagnetic actuation system to realize 3-D locomotion and steering within the digestive organs.^[17] In 2017, a dual hemisphere capsule robot from Dalian was mentioned that year as well.^[18] In 2018, a spiral robot were proposed, realizing controllable drug delivery.^[19] A three

symmetric magnetic legs capsule endoscope combining two innovated control system were reported as well last year.^[20] By the end of 2018, the sales of Ankon, which was the first company in the world to obtain the third type registration certificate for medical device of magnetron capsule gastroscopy system issued by China Food and Drug Administration (CFDA), had reached 169,000.

Table 1.3 lists some typical active endoscopes.

1.3 Brief Introduction of Wireless Communication System

Wireless communication is the transfer of information or power between two or more points that are not connected by an electrical conductor.^[21] With the rapid development of modern technology, wireless communication technology has achieved further development. Wireless access mode shows agility, high efficiency and quickness in the transmitting of data, image and characters without the limitation of time and space. It is more stable, reliable and flexible compared to cable transmission which provides unhindered long-time communication. However, it has certain confidentiality problems in application, such as being easier to get interception and interference in long distance transmission and cause information loss. Several mainstream wireless communication technologies are IrDA, Wireless Fidelity (Wi-Fi), ZigBee, Bluetooth, Ultra Wide Band (UWB), GPRS, and RFID.^[22] A general comparison is displayed in Table 1.4.

Almost all these communication types have something to do with Radio-frequency (RF), they all use RF to transmit data. For electromagnetic (EM), RF signals that realize radiation-based wireless power transformation (WPT) can at the same time be used for wireless communication.

Table 1.4 Comparison of Main Performance of Wireless Communication

Type	IrDA	Wi-Fi	ZigBee	Bluetooth	UWB	GPRS	RFID
Distance	<10m	<300m	<500m	<10m	<10m	∞	<2km
Rate	<4Mb/s	>2Mb/s	<250K b/s	<1Mb/s	>100M b/s	<171K b/s	1Kb/s
Frequency	900nm	2.4GHz	2.4GHz	2.4GHz	2.4GHz	<18000 MHz	<928M Hz
Development	Easy	Hard	Easy	Hard	Hard	Easy	Easy
Cost	Low	High	Low	Low	High	High	Low
Penetration	No	Strong	Weak	Weak	Weak	Strong	Strong

In addition to the demand for outstanding power and bandwidth efficiencies, the design of communication system of micro bionic robot must cope with the various degradations encountered such as adjacent channel interference, co-channel interference, fading, and multipath. Due to the fact that IrDA owns the disadvantage of being unable to work when being physically red and other types are either too expensive or too difficult to develop or can not work for long distance, a brand new low cost low power consumption wireless communication network is the aim of all researchers. Two frontiers are ZigBee and 433 MHz. The shortcoming of ZigBee that it is line of sight and its signal diffraction capability is limited prevents it from being applied in large-scale. This explains why it is not suitable for those communication requirements with certain physical barriers. 433 MHz which belongs to Industrial Scientific Medical works as a kind of supplement of ZigBee. Considerable penetration ability has brought about its wide application in smart furnishing, security, medical care and etc.^[23] Meanwhile, as the wireless signal will be inevitably weakened after penetrating the human body in the form of electromagnetic waves. Through precise calculation, 433 MHz was proved to satisfy the SAR demand and receiving power request.^[24] Since the industrial scientific medical frequency band does not require

authorization, a frequency can be considered as long as the transmission power is below 1 W, which makes sure that it will not interfere with other band.

1.4 Reviews on Wireless Communication System

Generally speaking, endoscopes all takes RF transmission in concern of specific demands mentioned above. The communication system of theses systems are all widely adopted secondary distributed system which is made up of a host computer and several inferior computers.

A lab from College of Information Technical Science, Nankai University realized a robotic control system for minimally invasive surgery robots with data collection and communication functions.

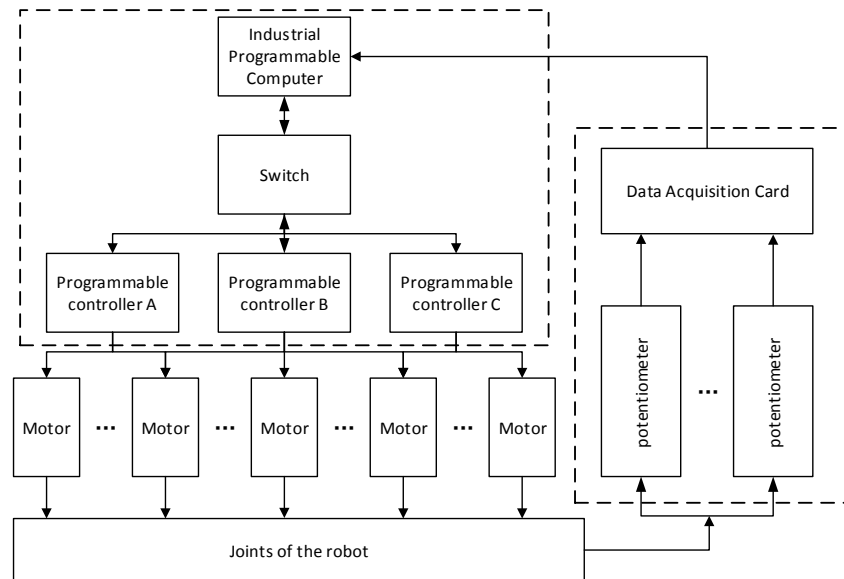


Figure 1.1: Hardware Structure of Control System

The system shown in Figure 1.1 is consisted of industrial programmable computer, programmable controllers and data acquisition module. The host computer connected each controller device through industrial internet. Such system fulfilled steady communication and real time control.^[25]

The wireless control system of Nanchang University took the nRF905 working at 433 MHz to conduct wireless communication. The host computer and MCU carried out serial communication through USB port and data transmission was completed via the Serial Peripheral Interface (SPI) port of MCU.^[26]

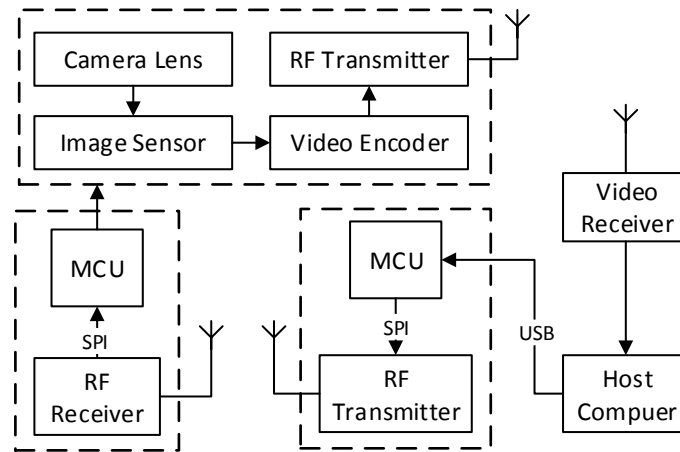


Figure 1.2: System Structure of the Wireless Capsule Endoscope

In 2003, a wireless capsule endoscope medical was introduced based on a single chip 2.4 GHz transceiver nRF24LE1 realizing wireless communication and image transition. The feature increased inner circuit consistency as well as lowers power consumption.^[27]

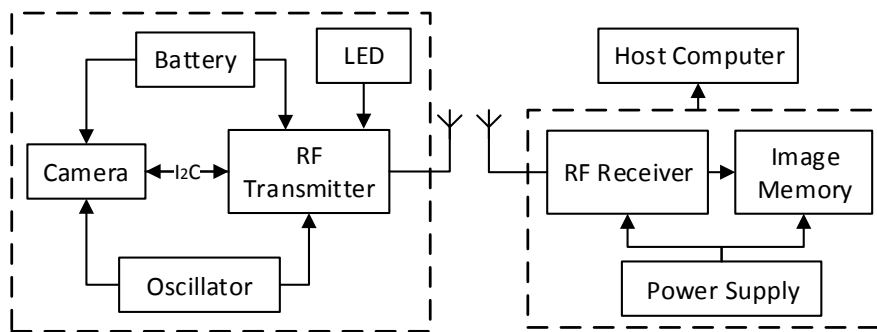


Figure 1.3: System Structure of the Wireless Capsule Endoscope

Similarly, the wireless communication applied in inner body soft robot conducted by Heng Wu, Taotao Zhou is made up of MSP430 and NRF24LE1 and the outside circuits at 2.4 GHz RF.^[24] The principle framework is shown in Figure 1.4.

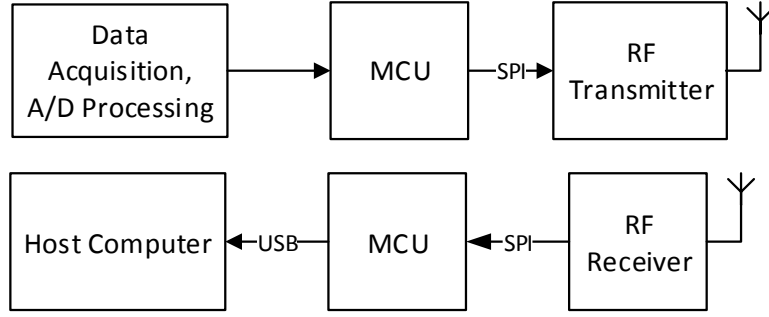


Figure 1.4: Principle Framework of the Inner Wireless Communication Module

Another system in Figure 1.5 with nRF24L01P+ controlled by ARM CortexTM-M4F working on 2.4 GHz took a similar structure as well.^[28] The protocol adopted was SPI and UART.

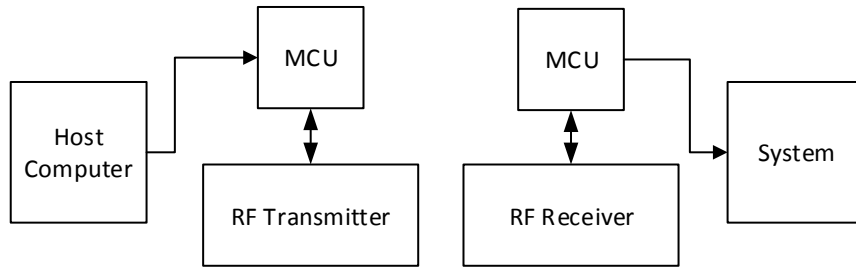


Figure 1.5: Framework Block Diagram

From previous documents, we can acknowledge that 433 MHz satisfies the International Commission on Non-Ionizing Radiation Protection (ICNIRP) safety standard as well as the sensitivity requirement of the intensity of the electromagnetic wave transmitted from the human body.^[26, 29] Silicon Laboratories' low-current, sub-GHz EZRadio transceiver SI4455 is adapted to work at 433 MHz. Its 3×3 mm package size with a low external bill of material (BOM) makes it efficient both in space and energy cost. The +13 dBm output power and excellent sensitivity of -116 dBm allows for a longer operation range. Its wireless development suit user interface module provides simplified programming options in an easy to use format that results in a quicker and lower risk development. The SI4455 communicates with the host MCU over a standard 4-wire SPI which can operate at a maximum of 10 MHz.

1.5 Objectives and Methodology

The whole robot system consists of the mechanism, the wireless power transmission system, the wireless communication system, the user interface and the supporting subsystem. This research mainly focuses on the wireless communication system. For sake of system replication and robustness, Hall sensors are introduced with related works to match up. Moreover, communication stability has long been a dilemma to extricate. Based on the assignment book and existing problems, the objectives of the project can be concluded into the following four parts:

1. Have an overall understanding of the whole robot system.
2. Design both the hardware and software of the wireless communication system with assembled Hall sensors.
3. Assemble all modules together, carry out relevant experiments, and debug the whole system.
4. Analyze the experimental results, optimize the system to improve the stability and reliability of the system.

The methodology can be divided into five parts, which corresponds to the five chapters followed.

In the first chapter, research background and significance, technology development from domestics and overseas and different wireless communication technologies are introduced at the very beginning. Relevant theoretical analysis papers, researches and achievements were studied on this topic to understand the composition and working principle of overall wireless communication systems.

The second chapter introduces the composition of the overall wireless communication system at first. Then, the hardware design of both the internal and the external module are explained separately in details. All elements are clearly presented and their particular uses are explained at great length.

The third chapter shows the software design logic with legible flowcharts of all submodules. Each submodule realizes a particular function to ensure the sound robot operation. The system is proved effective under direct power supply. Meanwhile, in consideration of integrity, readability as well as aesthetics in practical applications, an integrated interactive interface is programmed for convenience.

Most importantly, this research has improved the stability of the wireless communication system of micro bionic robot for noninvasive gastrointestinal diagnosis. The fifth chapter mainly discusses the problems during the assembly coordination. Aiming at all kinds of unstable communication situations under wireless power supply, experiments were designed and carried out from various aspects. Perfected power transmitter offers larger power transmitted, energy management circuit buffers the voltage plummet, multi-coil transmission structure improves the transmission efficiency, and new voltage regulator chip saves the power consumed. Based on these results and achievements, the crux of the matter is figured out. The optimized program fundamentally solved the long perplexing trouble.

The final chapter analyzes the experimental results in detail and gives some suggestion on the future work.

Chapter Two Hardware Design of the Wireless Communication System

The wireless communication system mainly includes host computer, external communication module, internal communication module, internal control module and the video module. Circuits design covers serial communication, wireless communication, motor driving, position detection, current detection and some other parts. The working principle and the construction of the entire wireless communication system can be visually displayed in Figure 2.1 in which dotted line refers to wireless communication and solid one refers to wired communication.

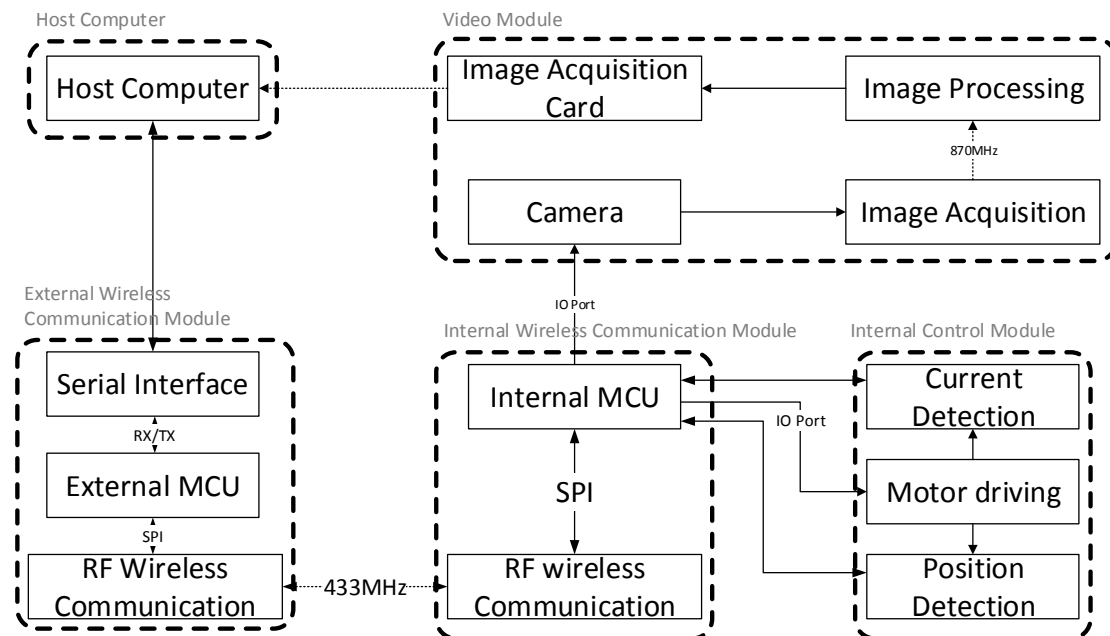


Figure 2.1: Wireless Communication and Control System Overview

User send control commands through the host computer which works as the operation terminal. It decodes the commands and send them to the external wireless communication module through RS-232 serial interface. The external PIC24 series

microcontroller unit (MCU), working as a transfer station, realizes bidirectional communication control between MCU and host computer via RX/TX serial port. Serial Peripheral Interface (SPI) actualizes the control of sub-GHz wireless transceiver chip SI4455 by MCU. Industrial Scientific Medical (ISM) 433 MHz were chosen for radio receiving and transmitting in virtue of SI4455 and peripheral circuits. Vice versa, commands are transmitted to the internal communication module. Internal MCU controls corresponding I/O ports to realize specific functions according to the commands decoded. Current detection and position detection module are for real-time monitoring of robot motion and valid control. MCU controls the on-off of the camera. The camera MCU configures parameters by Serial Camera Control Bus (SCCB) control bus and emit National Television Standards Committee (NTSC) standard analog image signal in 870 MHz ISM frequency. After image processing, images are transported to the image acquisition card to demonstrate the intestinal environment for diagnosis after format transition and compression.

Wireless communication module can be roughly classified into the internal module and the external module.

2.1 Design of the External Wireless Communication Module

The external one mainly deals with the serial interface submodule and the wireless communication submodule.

A. The serial interface submodule

For the host computer adopts RS-232 logic voltage signal standard which differs from what the MCU with serial communication function took, direct connection is unattainable and a voltage signal converter chip is indispensable. Figure 2.2 offers the schematic of the serial interface submodule. The voltage signal converter chip MAX3232CSE which adopts the design of standard serial interface RS-232 is chosen. Its RX/TX ports are connected to the MCU PIC24F16KA102 and its 13/14 ports are

connected to pin 2/3 of the D-sub 9 connector attached to the host computer to realize communication. Pin 2 receives data and pin 3 transmits data.

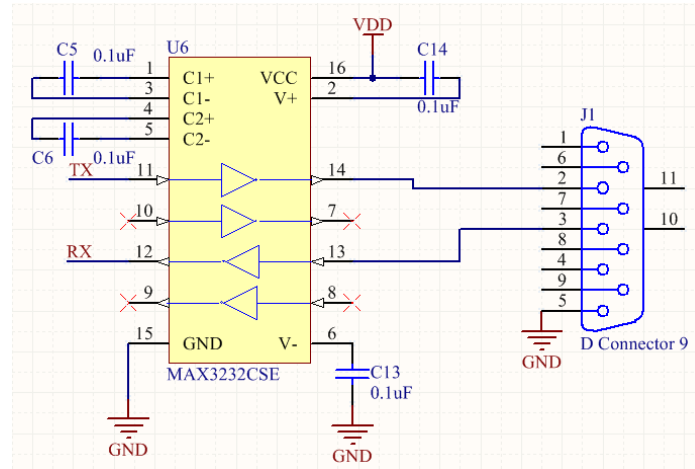


Figure 2.2: Schematic of Serial Interface Submodule

B. The wireless communication submodule

The SI4455 communication chip covers the frequency range from 283 MHz to 960 MHz and 433 MHz is elected here. Detailed reason is mentioned above. Its -40 ~ +13 dBm output power range and -116 dBm receive sensitivity broaden its working range. The demodulated signal is output to the system MCU through a programmable General-purpose input/output (GPIO) or via the standard SPI bus by reading the 64-byte RX first in first out (FIFO) storage. Its schematic is Figure 2.3. SI4455 uses a 30 MHz crystal oscillator with a fast start-up time of less than 250 μ s and communicate with MCU by SPI interface. Data sheet indicates that SDN port controls power on-off mode of the chip, nIRQ considers interrupt states, nSEL provides select/enable function for 4-line serial data bus and SDI, SDO separately refers to serial data input and output. Figure 4 indicates its application circuit.

The SI4455 operates as a time division duplexing (TDD) transceiver where the device alternately transmits and receive data packets at a time. So, operating mode should be properly set before transition or reception to form a sensible time series and provide stable communication.

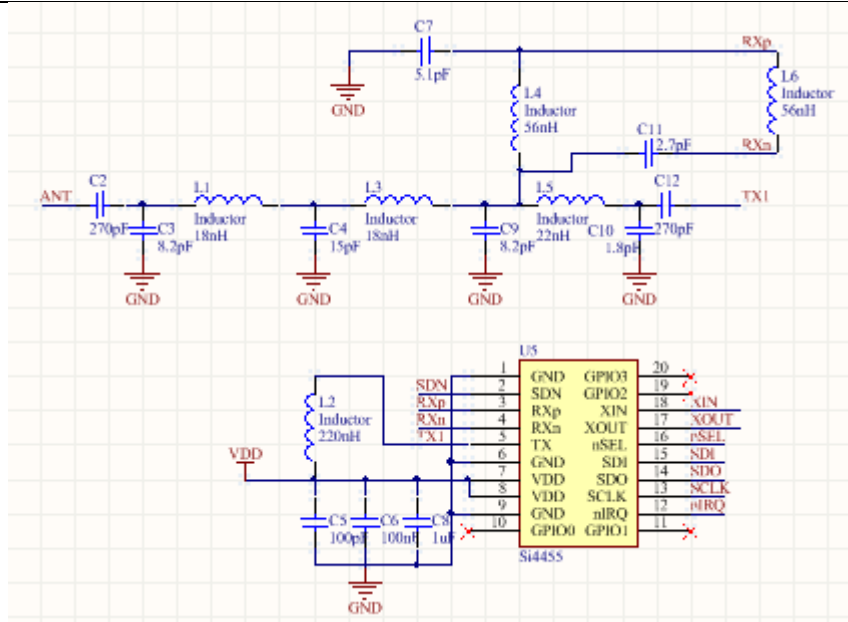


Figure 2.3: Schematic of SI4455 Communication Circuit

The whole circuit design of the internal control module is shown in Figure 2.4.

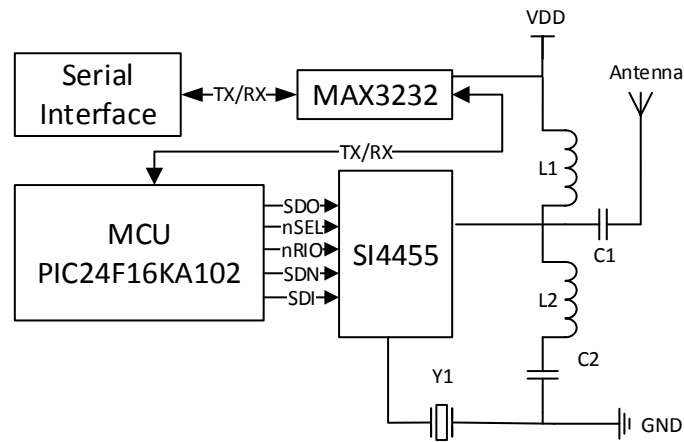
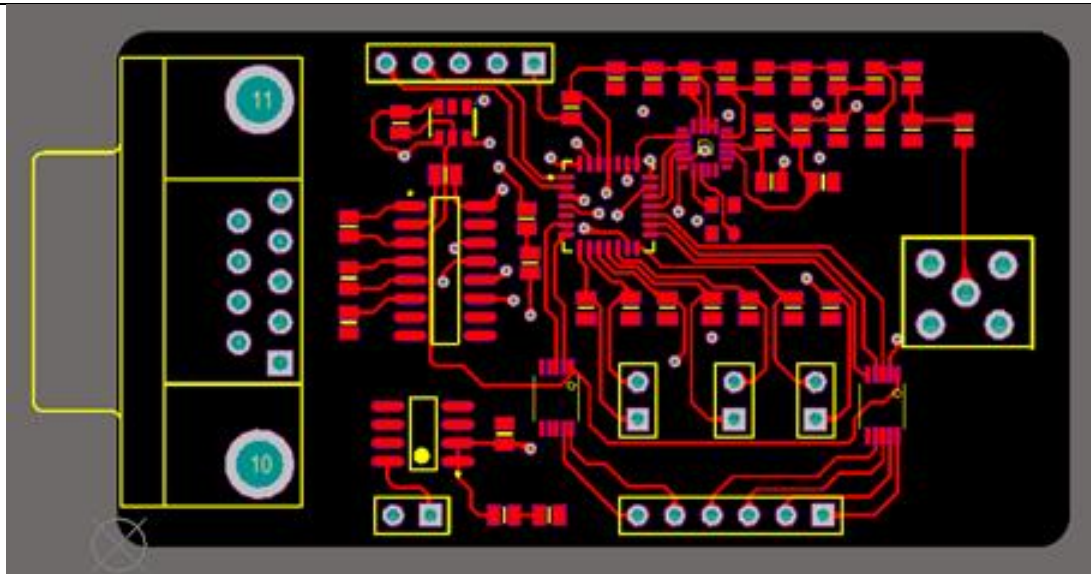


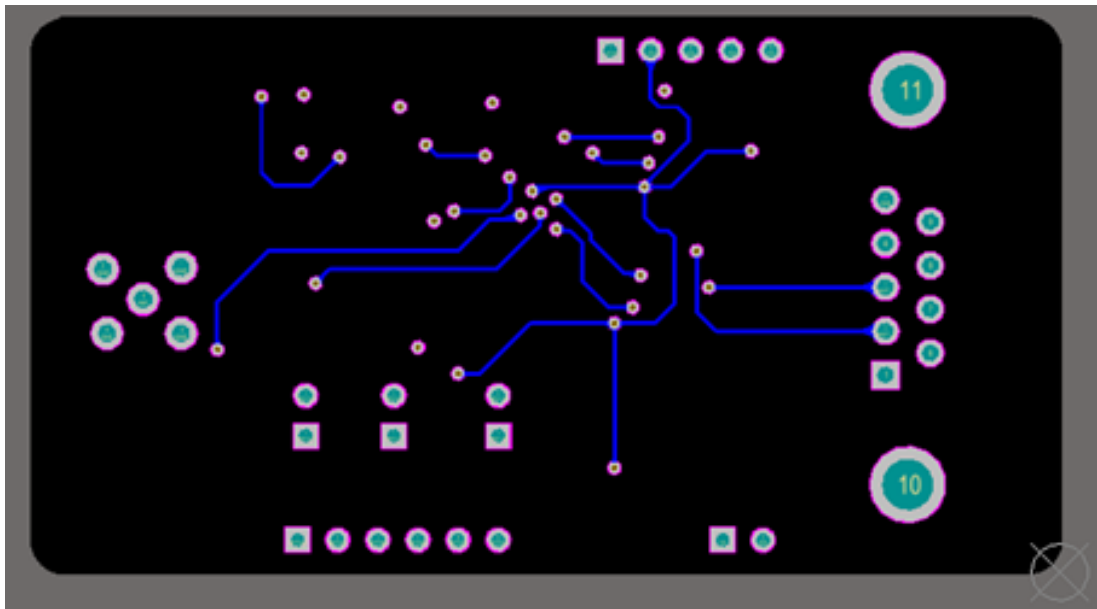
Figure 2.4: Whole Circuit Design of the External Wireless Communication Module

For the convenience of robot debugging, the transmitting PCB board also includes PIC24 series MCU, micropower low dropout regulator, current-sense amplifier and 2-channel motor drive.

The whole board is shown in Figure 2.5 in which (a) (b) separately shows its top and bottom layer.



(a)



(b)

Figure 2.5: PCB Board Design of the External Wireless Communication Module

Figure 2.6 demonstrates the front of the external wireless communication module.
 Figure 2.7 displays the integrated control box and the back of the PCB board.

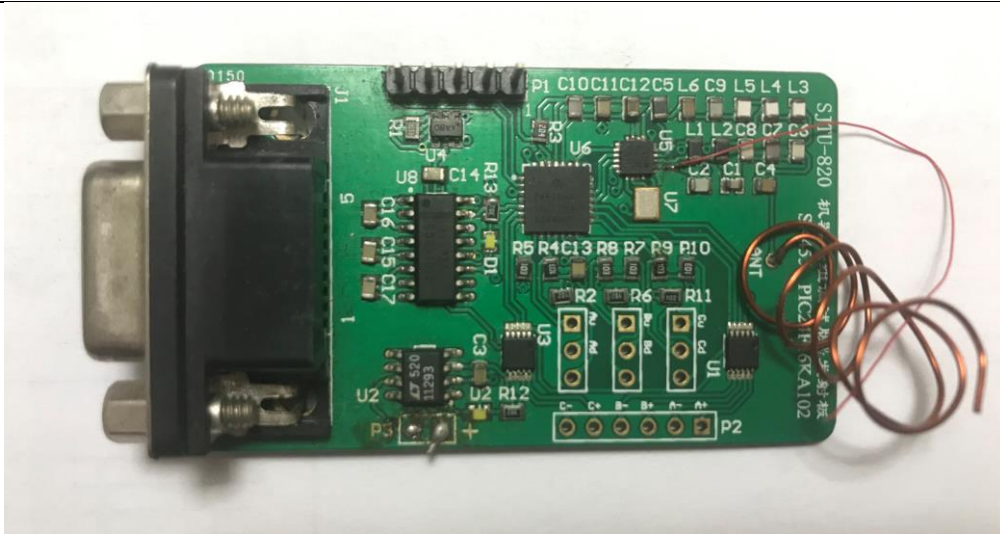


Figure 2.6: Completed PCB Board of the External Wireless Communication Module

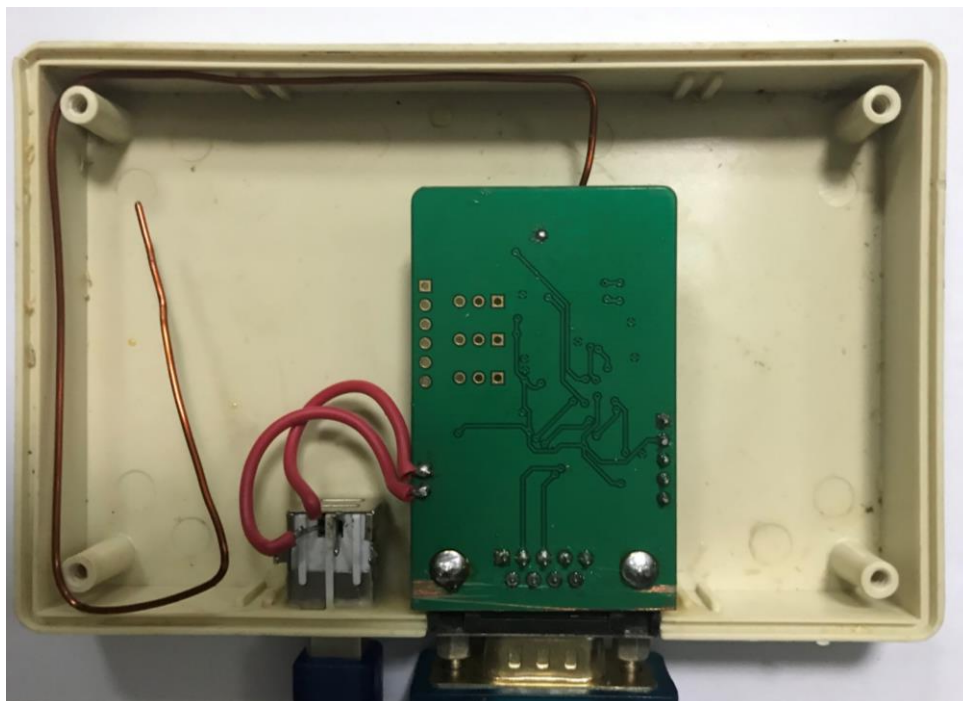


Figure 2.7: Launch Control Box

2.2 Design of the Internal Wireless Communication Module

The original board used PIC16F690 in concern of size demand. However, since

six more I/O ports are needed to receive the outputs from the Hall sensors, PIC24F16KA102 is chosen to replace the original MCU. The new MCU is larger than the original one and the circuit is different, so elements should be reorganized. The board was redesigned. In addition, for the convenience of testing and welding, a test board shown later in Figure 3.3 was also designed. Figure 2.8 (a) is the original board and (b) is the redesigned board.

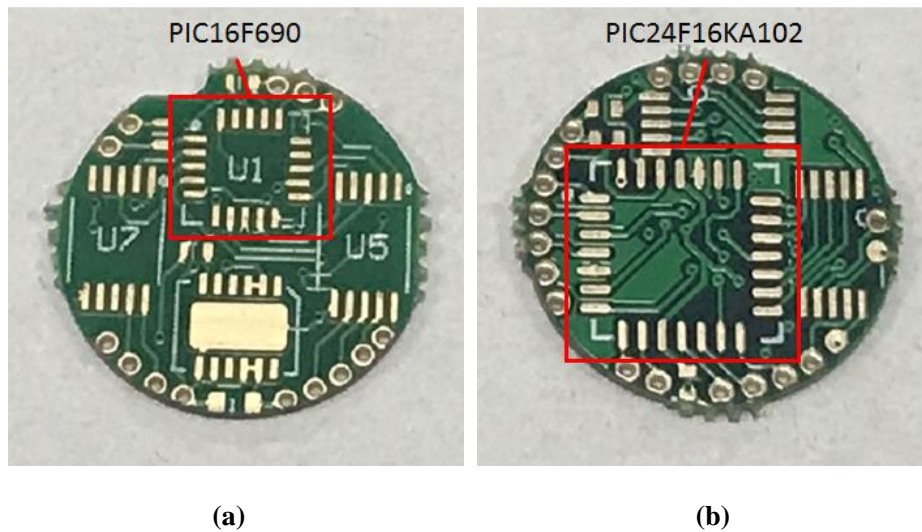


Figure 2.8: The PCB boards of the Internal and External Wireless Communication Module

The internal part mainly deals with the wireless communication submodule. For internal wireless communication module, PIC24F16KA102 whose 24 I/O ports fitly meet the design demand with assembled Hall sensors and the wireless receiver chip are all the same as mentioned in the external submodule. Figure 2.9 demonstrates the schematic of MCU whose body is 6×6 mm. It owns brown-out reset (BOR) characteristic with three programmable trip points which can be disabled in ‘Sleep’ state. In-circuit serial programming and in-circuit debug are done via two pins. It should be pointed out that all device pins have a maximum voltage of 3.6 V and are not 5 V tolerant. Capacitor C1 aims at decoupling. The \overline{MCLR} pin provides two specific function: device reset, and device programming and debugging which is not required in end application, so it is directly connected to VDD.

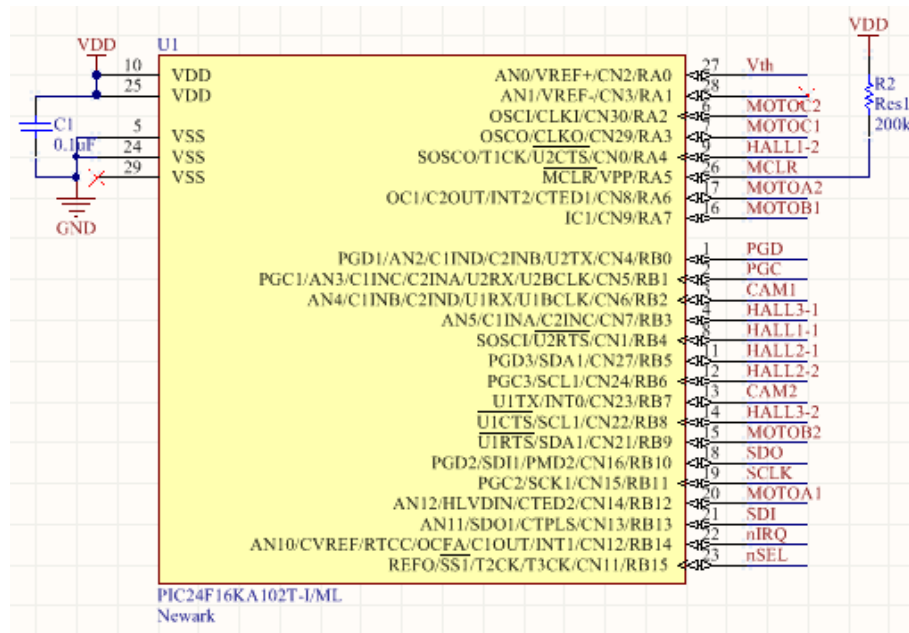


Figure 2.9: Schematic of PIC24F16KA102

The internal control submodule mainly includes motor control, current detection and position detection submodules.

A. Motor control submodule

The motor used is coreless, synchronous servo motors whose length is 12 mm and diameter is 4 mm. Its nominal voltage is 3.3 V and unload current is 30 mA. Its rotational speed is 40000 rpm without a load.

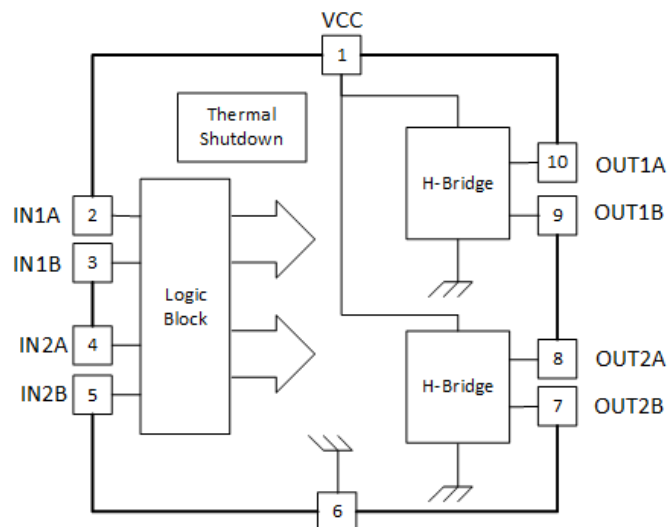


Figure 2.10 Typical Application Circuit of AT5550

For the reason that 18 mA high-current sink/source on all I/O pins is too small to directly drive the motors, so AT5550 2-channel H-bridge motor drives are used. Its package size is 3×4.9 mm. Figure 2.10 shows its typical application circuit.

Absolute maximum ratings are clearly listed in the datasheet, marking its 2~5.5 V supply voltage, 800 mA maximum output current, -400~400 mA H-bridge output current, 870 mW power dissipation, 0~100 kHz and 2 KV electrostatic discharge sensitivity (ESDS) for human body model.

Table 2.1: Input-output Logic Table of AT5550

Input				Output				Mode
IN1A	IN1B	IN2A	IN2B	OUT1A	OUT1B	OUT2A	OUT2B	
L	L	L	L	Z	Z	Z	Z	Standby
H	L	L	L	H	L	Z	Z	
H	L	H	L	H	L	H	L	
L	L	H	L	Z	Z	H	L	
L	H	H	L	L	H	H	L	1,2 phase excitation
L	H	L	L	L	H	Z	Z	
L	H	L	H	L	H	L	H	
L	L	L	H	Z	Z	L	H	
H	L	L	H	H	L	L	H	Keep the previous output state
H	H							
		H	H					

Input-output logic table is listed in Table 2.1.

As two radial motors, one axial motor and a video module are to be driven, four independent channels are needed which means two chips are just right for application demand. Figure 2.11 displays the schematic.

When the robot is working, rotor lock will cause overcurrent, doing harm to the motor. Poor load capacity of coreless motor cannot prevent the structure from getting stuck. This consequently prejudices the performance of the wireless communication module and the whole system. Generally speaking, three causations generate rotor lock. One is intestinal resistance. Another is mechanism restriction at the beginning and end of each movement. The last one is other mechanism lock happened during the

movement.

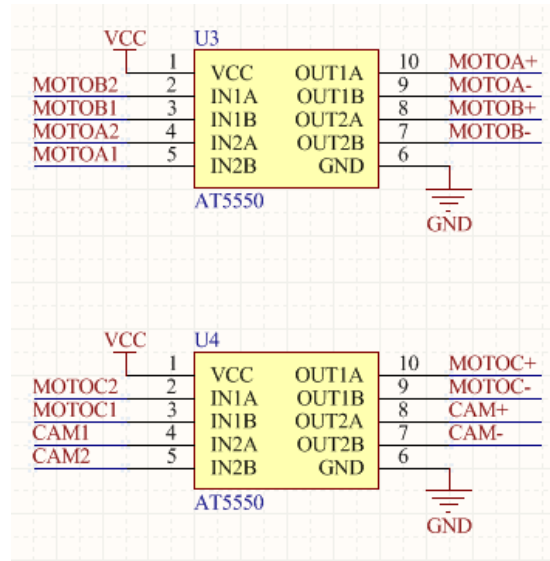


Figure 2.11: Schematic of Motor Control Submodule

B. Current detection submodule

This submodule is designed to solve the first cause. The current is monitored to shut down the motor or conduct next operation when overcurrent occurs. By doing this, the life of motors can be prolonged. Low-cost, high-side, 3×3 mm current-sense amplifier MAX4173F available in a tiny SOT23-6 package is used to amplify the current flowing through sampling resistance and send the value to AD sampling port of the MCU.

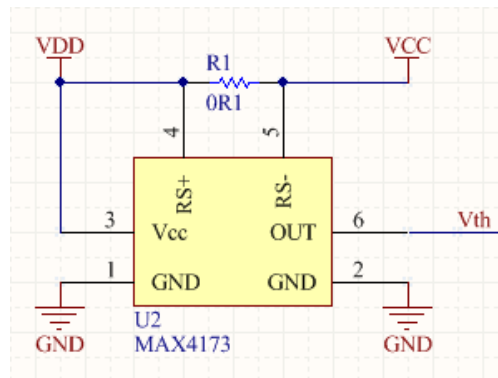


Figure 2.12: Schematic of Current Detection Submodule

Figure 2.12 is the schematic of current detection submodule in which VDD refers

to power input and VCC stands for load power supply. For this submodule detects the working current of the motors, VCC is the power input of AT5550 and the current flowing through the sampling resistor R_1 is the motor driving current.

It features voltage output that cuts down the requirement for gain-setting resistors, making it ideal for critical current monitoring. It operates from a single 3~28 V voltage supply, drawing 420 μ A supply current. With +50V/V gain version chosen, its gain accuracy and bandwidth is separately $\pm 2.5\%$ and 1.4 MHz. According to recommended component values table, full-scale load current I_{load} is set to be 1A with 100 m Ω current-sense resistor R_{sense} as the output voltage is 0~3 V and the working current of the motor is 0~400 mA.

C. Position detection submodule

With single current detection module, rotor lock can not be completely avoided. Every time the current module detects the rotor lock, it has already taken place. Even though the motor is shut down after detecting the overcurrent, its response is not considerably effective. What's more, the threshold of each motor can be different. So it can not be the only criteria. So position detection submodule is proposed to act in advance before reaching limit positions and provide double protection.

Mechanism position detection measurement is usually divided into contact and non-contact types. Contact ones detects the position through the contact between the shift common terminal and the stiff elastic elements. Three terminals are there in one unit for detection. When common terminal meets the elastic element at the start or end of the movement, the output jumps accordingly from low to high. This kind of method enjoys simple structure but suffers poor stability and persistence.

Non-contact ones are usually realized with Hall sensor and permanent magnet settled separately at the shift terminal and the stiff terminal of the mechanism. When the sensor gets closer to the permanent magnet, the magnetic field around gets stronger. When the magnetic field intensity reaches the threshold set, the output of the Hall sensor immediately changes. Hall sensor enjoys wonderful isolation which

prevents disturbance and provides ideal stability as well as persistence.

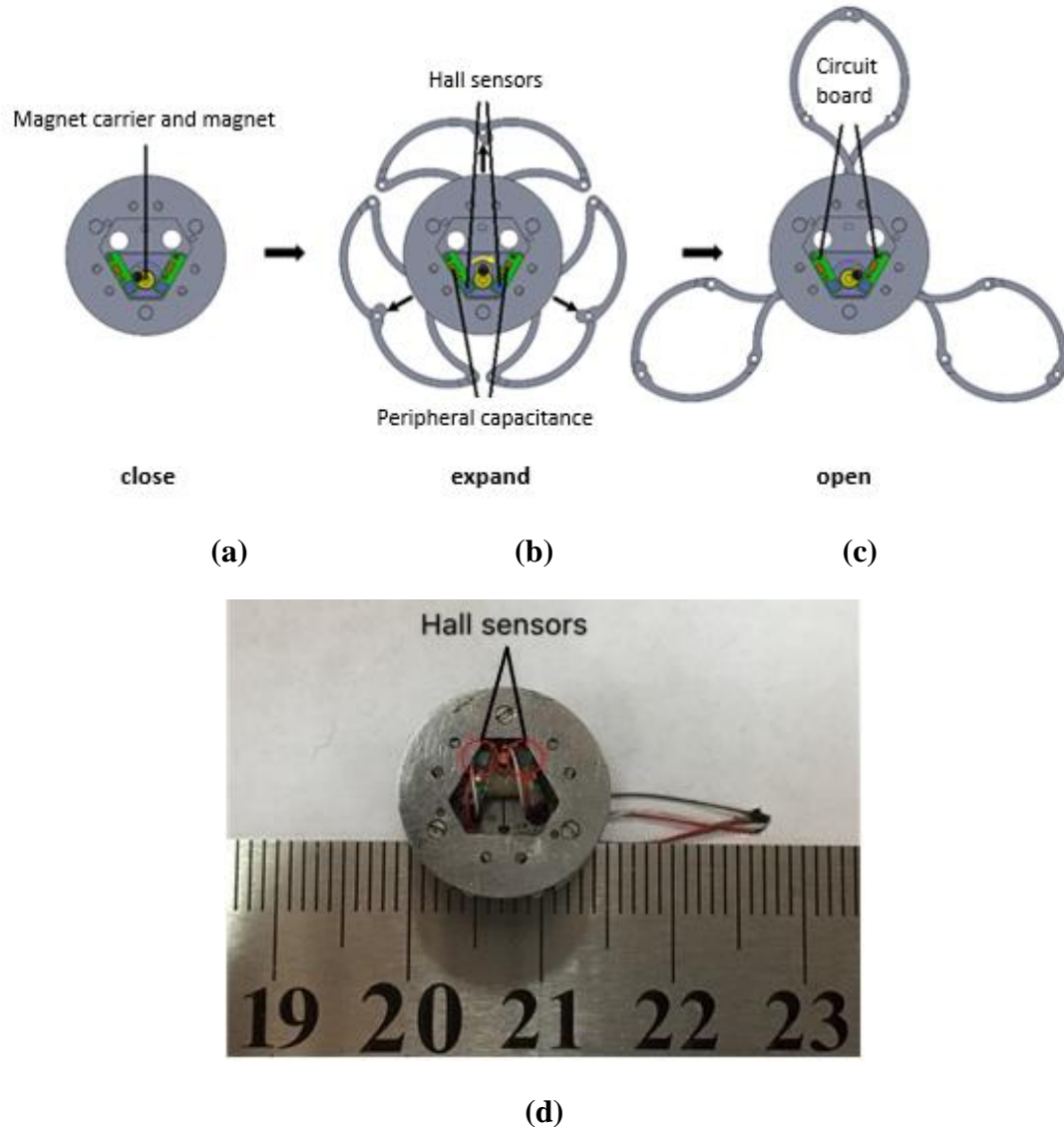


Figure 2.13: Mechanism of the Position Detection Module

Figure 2.13 (a), (b), (c) describes how the mechanism works from close to open. This procedure decides why in each motion mechanism two Hall sensors should cooperate in pair. Six Hall sensors are used for two limit positions of each motion mechanism. Figure 2.13 (d) is the entity of the Hall element settled onto the mechanism.

The schematic of ultra-sensitive, pole-independent Hall-effect switch A1172 with a latched digital output is performed in Figure 2.14.

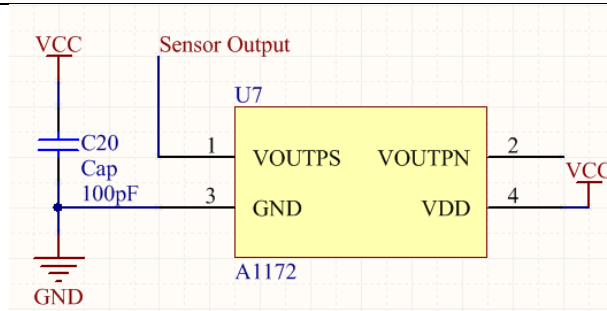


Figure 2.14: Schematic of Position Detection Module

A1172 insensitive to physical stress, has no magnetic orientation required during assembly. It offers magnetically optimized solutions, suitable for applications. The 1 mm by 1 mm by 0.5 mm small package meets the limited space demand of the robot. Its 1.65~3.5 V operating supply voltage and special clocking algorithm reduce the average operating power requirements to less than 15 μ W with a 2.75 V supply. Additionally, dynamic offset cancellation using chopper stabilization fulfills improved stability, which reduces the residual offset voltage.

The pin VOUTPS is connected to the I/O port of the MCU to control the startup and shutdown of the motors. Its original output signal is high and it will jump to low when the strong enough magnetic field is detected thus realizes position detecting purpose.

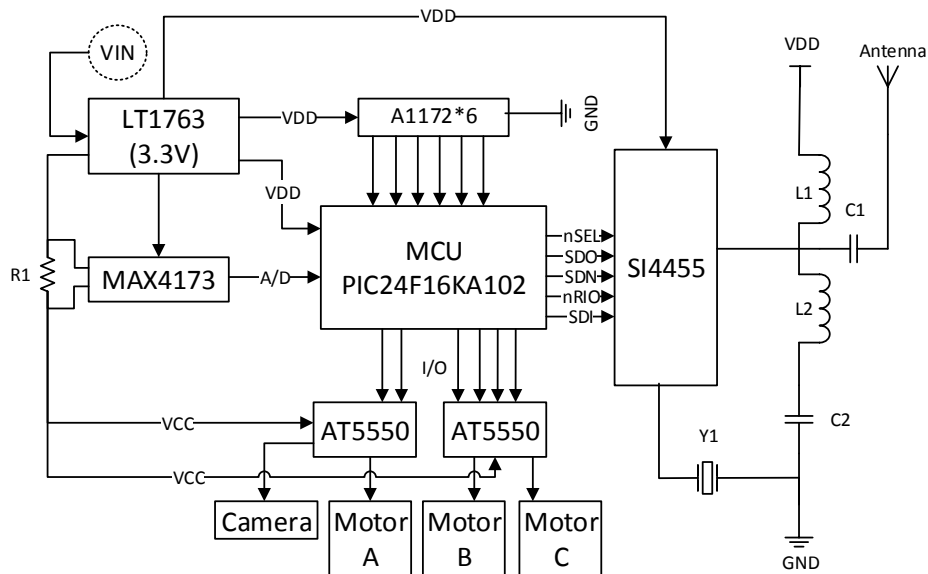


Figure 2.15: Whole Circuit Design of the Internal Wireless Communication Module

The whole circuit design of the internal control module is shown in Figure 2.15.

Figure 2.16 exhibits the whole PCB board. Figure 2.16 (a) shows its top layer and Figure 2.16 (b) shows its bottom layer.

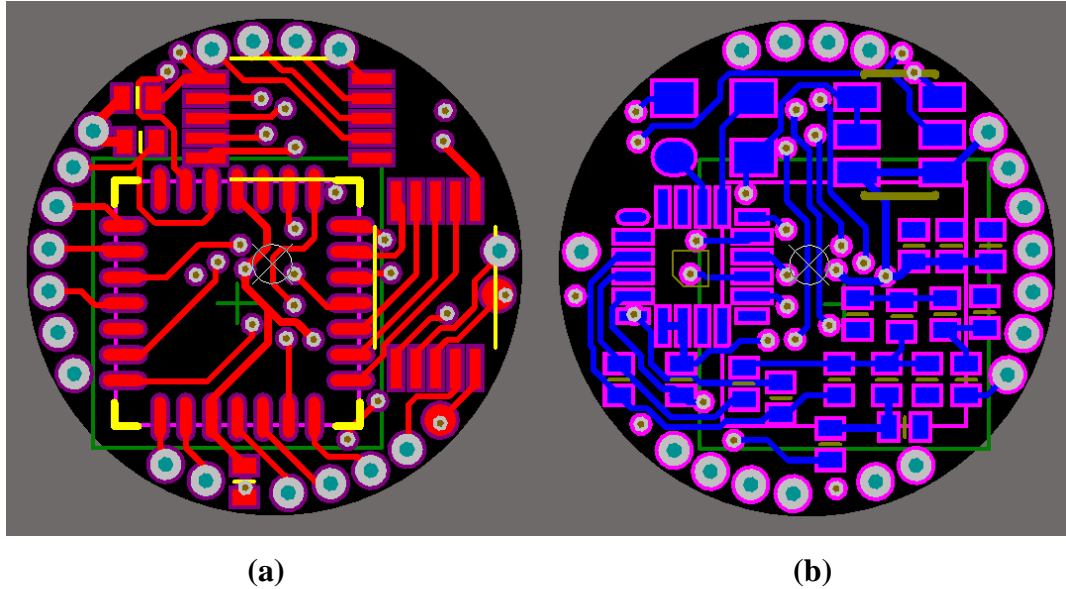


Figure 2.16: PCB Board Design of the Internal Wireless Communication Module

Figure 2.17 is its PCB board entity in which (a) and (b) separately shows the front and back of its entity.

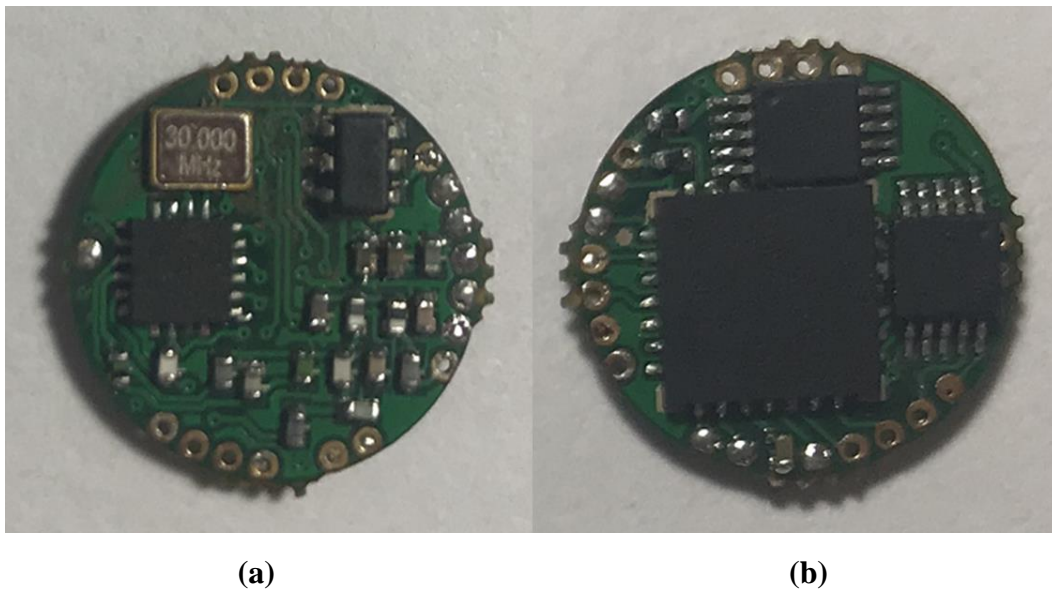


Figure 2.17: Completed PCB Board of the Internal Wireless Communication Module

Chapter Three Software Design of the Wireless Communication System

All the wireless communication programming is developed under the MPLAB IDE environment with MPLAB C30 compiler. As mentioned before, the MCUs of both internal and external module are all PIC24F16KA102 and sub-GHz EZRadio transceivers are all SI4455, following SPI communication protocol.

3.1 Programming of the External Communication Module

As mentioned above in Chapter 1.4, the host computer communicates with the external MCU with the help of voltage signal converter chip MAX3232. The MCU and the MAX3232 are connected through Universal Asynchronous Receiver/Transmitter (UART) with Baud rate 9600. Figure 3.1 indicates how the program of the external communication module works. After initialization at the very beginning, the status of SI4455 is continuously checked. As soon as the data sent from serial interface is received, it is sent both to the internal communication module through internal SI4455 and back to the host computer. Meanwhile, the external SI4455 sends the data received from the internal SI4455 to the host computer. So, a successful communication case will have 32 byte data in the receive buffer on the screen of the host computer. The overall flowchart of the external communication module is displayed in Figure 3.1.

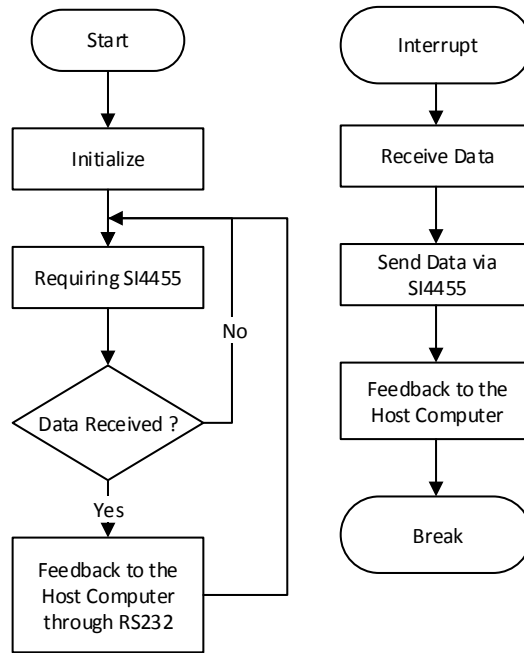


Figure 3.1: Overall Flowchart of the External Communication Module

The data sent is set at the length of 16 bytes and the outcomes can be listed as followed. If the feedback is two groups of 16-byte data same as what is sent, it means that the wireless communication between the host computer and the internal wireless communication works perfectly. If only the former 16 bytes are the same as what is sent with later bytes less than 16 bytes different, this indicates that the communication between the host computer and the external communication module achieves success. However, the communication between the external and the internal communication module is stuck in failure. 16-byte data different returned means that the host computer cannot communicate with the external module. If the data returned is fewer than 16 bytes, the communication between the host computer and the external communication module gets complete failure. Such kind of programming and analysis helps a lot in debugging.

Table 3.1: Meanings of Each Byte of the Control Words

	byte 00	byte 01	byte 02	byte 03	byte 04	byte 05	byte 06	byte 07
value	AA	80	02	30	02	30	02	30
meaning	flag	command	Limit current A		Limit current B		Limit current C	

Table 3.1

	byte 08	byte 09	byte 10	byte 11	byte 12	byte 13	byte 14	byte 15
value	01	01	01	00	00	00	00	AA
meaning	Hall flag A	Hall flag B	Hall flag C	default	default	default	default	flag

The meaning of each byte of the control words are explained in Table 3.1.

Byte 00 and byte 15 works as flags to check data validity. Byte 01 contains the command message. Each two bytes from byte 02 to 07 refers to the threshold of limit current of different motors. As the installation of Hall sensors are of huge difficulty and little position error brings unneglectable consequence, once the Hall element deviates from the expected trajectory, it will be of extreme complication to repair and adjust. Thus, byte 08 to byte 10 are used as flags to choose whether the program of Hall element should be conducted or not. So that, when the Hall sensor goes wrong, there is no need to disassemble the robot with lots efforts, the relevant part can still work with single current detection module to increase the practicability of the whole robot. Byte 11 to byte 14 is left default here for future convenience.

In details, the relationship between byte 01 and the command of real meanings is displayed in Table 3.2.

Table 3.2: Meanings of Byte 01

Byte 01	Command
80	Open the front radial motion mechanism
82	Close the front radial motion mechanism
A0	Open the axial motion mechanism
A4	Close the axial motion mechanism
C0	Open the rear radial motion mechanism
C4	Close the rear radial motion mechanism
E0	Continuously moving forward
F0	Continuously moving backward
FF	Reset

Based on the mechanical motion principle in Figure 3.2, continuous movements are realized through rigorous logic programming.

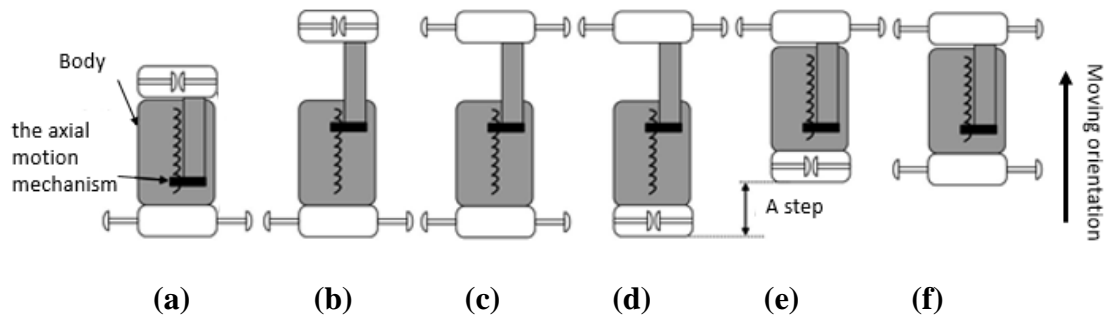


Figure 3.2: Mechanical Motion Principle of the Inchworm-like Robot

Take continuously moving forward as an example, six steps are there in one cycle. First of all, the robot closes its front radial motion mechanism and open its rear mechanism to stop at its current location. Secondly, the axial motion mechanism extends. So the front moves forwards. Then, the front motion mechanism opens followed by closing the rear one. After that, the axial motion mechanism draws back with the front one open, keeping the robot stay at a step forward. In the end, the rear one opens to expand the intestine and realizes detention. The state of motion is recorded in the Electrically Erasable Programmable Read Only Memory (EEPROM). Position detection and current detection is also included in every single movement. Continuously moving backward works similarly vice versa.

As for byte 02 to byte 07, two bytes in pairs stands for the limit current. The number here does not directly equals to the real current. It only works as a relative value. Through setting a breakpoint, monitoring the current on the board, the current value under different working circumstances can be figured out.

Under normal working condition, the current detected in the experiments ranges generally from '0x0020' to '0x0040'. As shown in Figure 3.3, the threshold '0x0230' is chosen to be the critical point to enable the motor to serve for entire movement on one hand and prevent motor lock caused insufficient power supply on the other hand in theory.

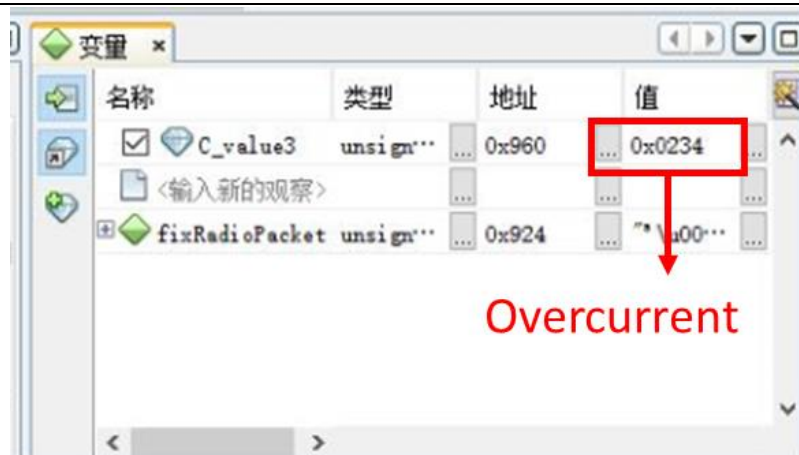


Figure 3.3: The Screenshot Showing the Overcurrent Value

Since all three motors are of same type and the currents monitored show little difference, the thresholds are kept equal for all three.

3.2 Programming of the Internal Communication Module

At the very beginning, the program initializes the MCU, the I/O port, the SPI, the Analog-to-Digital Converter (ADC), configures the SI4455, enables the watchdog timer and defines the interface between RF transceiver and MCU. Signals are continuously transmitted and received during the while loop and then conduct the corresponding instructions according to the signals. The programming is designed in consideration of the problems met in application. Figure 3.4 displays the overall flowchart of the internal communication module.

Being powered on, initialization will be first done. Then, the internal wireless communication module will be at a standby state, waiting to receive commands. Using nIRQ to monitor the current state, as soon as an interrupt event occurs, the program will read the interrupt status registers and clear the pending ones.

As long as the radio packet is sent successfully, the text received will be packed and whether the control words meets the communication protocol will be checked first of all. With the success of data validity, all data will be saved with check words removed and flags will be set accordingly. By doing this, the robot can execute

different commands accordingly. If there occurs any failure during the process, the FIFO will be reset to start from the very beginning, staying at the standby state for next command.

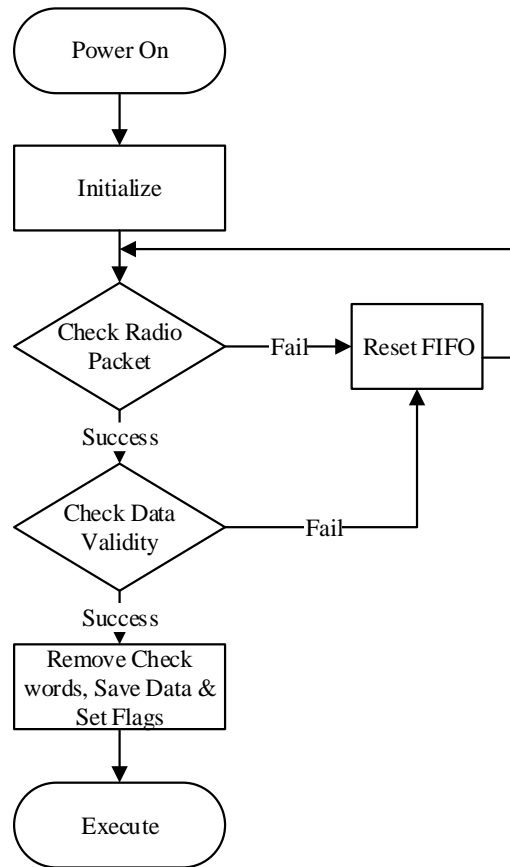


Figure 3.4: Overall Flowchart of the Internal Communication Module

A. Position detection submodule

Moving in the intestine, overcurrent always occur when endoscope comes to the end of its movement. By adopting double signal feedback control method whose logic is described in Figure 3.5, the priority of the position detection which should be set higher than the current detection is realized.

When conducting a command, the outputs of the Hall sensors, namely the position detection, should first be done. With low output indicates reaching the limit position, the robot should stop or answer the next command. Otherwise, current detection should be followed, making sure that the present current detected does not exceed the threshold value set. If excesses happen, it means that the motor is rotor

locked, then the robot should stop or answer the next command. If not, the action should continue and move on with position detection. The position detection submodule is added after all functions are realized, so during the testing process, this part of the program is noted by setting part of the control words sent.

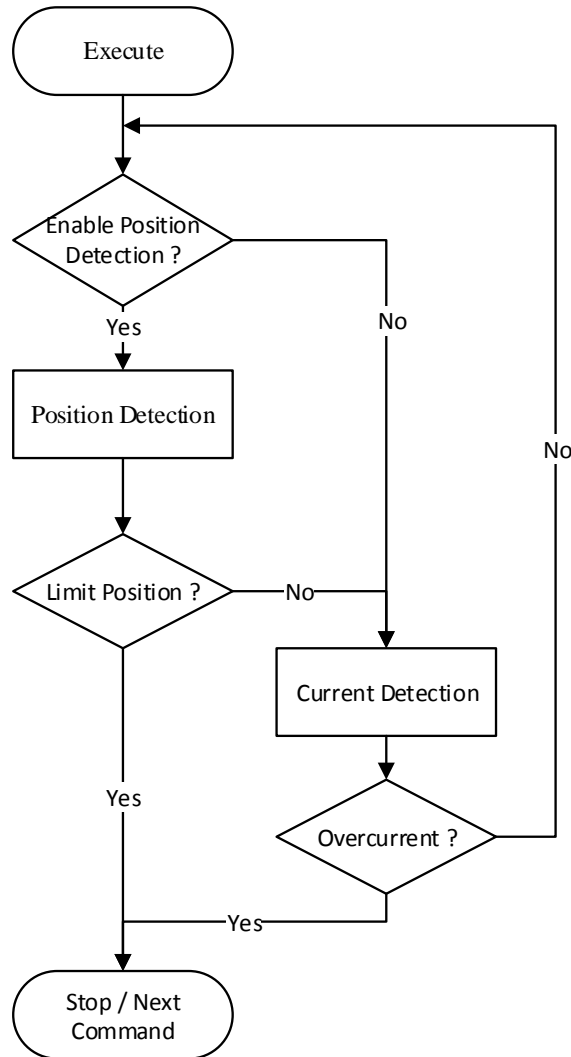


Figure 3.5: Flowchart of the Position Detection Submodule

B. Current detection submodule

Meanwhile, for the current detection submodule, the current detected should be processed by filtering to avoid false judgment caused by current fluctuations, noises and peaks. Eight samplings are included in one detection as shown in Figure 3.6. To avoid the interference brought by relatively high startup current, the current detection submodule conducts sampling after a delay, namely the overcurrent time which can be

set in the control words sent. By setting the time to zero, its real default time is the instruction cycle clock which equals two times the input oscillator time base period.

In Figure 3.6, I_m refers to the current threshold and I_0 refers to the average of eight sampled current values.

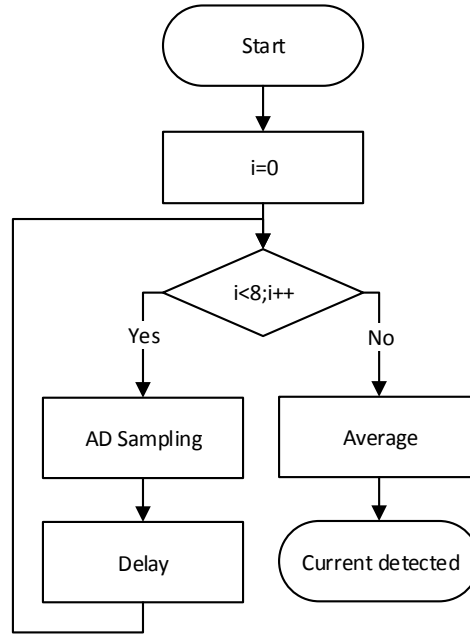


Figure 3.6: Flowchart of the Current Detection Submodule

As Figure 3.7 describes, comparing the average current value to the current limit set, the robot will stop or execute next command when overcurrent occurs. Otherwise, the program will run the detection cycle repeatedly until overcurrent occurs or the robot comes to the end of its movement.

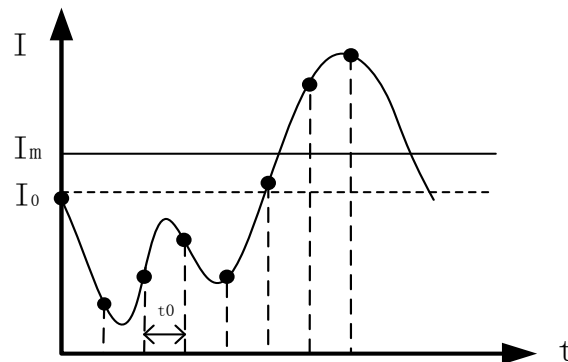


Figure 3.7: Overcurrent Sampling

3.3 Hardware and Software Debugging

After the PCB board was welded, tests were done with multimeter to make sure there was no cold solder joint or misplaced elements. Then, tests should be done step by step for debugging.

The test board in Figure 3.8 was designed for debugging convenience.

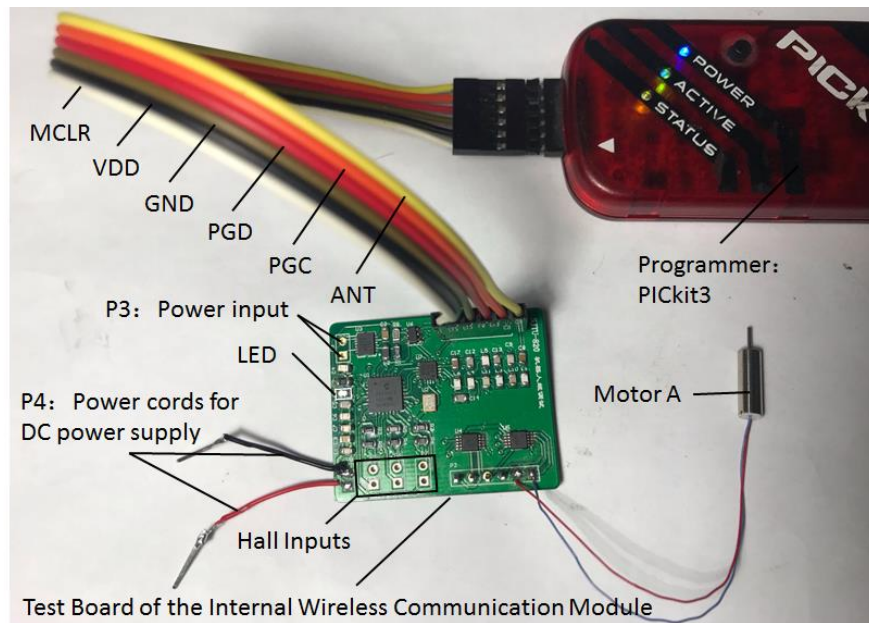


Figure 3.8: Test Board of the Internal Wireless Communication Module

The three pairs of pins at the bottom left corner is for tests of Hall sensors. They are connected to the ground by default. Two power cords are for the convenience of testing under DC power supply circumstances. The top left pins P3 is the power input from the rectifier board, which is usually over 5~7 V. The P4 at the bottom left corner is used to check whether the output of the voltage regulator is maintained around 3.3 V. The LED indicates whether the voltage output is ideal.

First, as shown in Figure 3.8, the internal wireless communication board should be connected to the PICKIT3 programmer through the six cords on the top right corner.

Once the connection succeeded, 'PICkit3 Connected.' could be seen on the screen. With the successful connection between the MCU and the host computer, the feedback of sending 16 bytes command is at least 15 bytes. 15 bytes feedback is abnormal and can be fixed by repowering up the external wireless communication board. For the six cords, MCLR refers to Master Clear which provides fulfills device reset as well as device programming and debugging. VDD and GND is the power and the ground. PGD refers to programming data while PGC refers to programming clock. They are used for in-circuit serial programming and debugging purposes. ANT, the antenna is for increasing receiving sensitivity.

32 bytes feedback suggests successful communication through the RF transceiver SI4455. If the feedback is only 16 bytes or 31 bytes, there must be something wrong with the RF transceiver. To test the motor drivers, different commands should be sent and check whether the test motor changes its rotation direction. To test whether the current detection module functions well, the rotor should be locked in purpose. If the rotor stopped, this means the module works well. Under DC power supply, the current can be seen to be 0.1 A.

3.4 Programming of the Integrated Interactive Interface

For the convenience and integrity of controlling the micro bionic robot, a delicate integrated interactive interface is of great importance. With a nice integrated interactive interface, users like doctors and nurse will have no need to enter long, complicated confusing and error-prone control words. All operations can be done with ease. The interface is complied by Labview and Figure 3.9 demonstrates the Login interface.



Figure 3.9: Login Interface of the Integrated Interactive Interface

Figure 3.10 describes the operation interface. The program is finally generated into an executable application.

Using this application, the robot can act accordingly based on the buttons clicked and the values set. A tab on the front panel is used to realize page skipping.

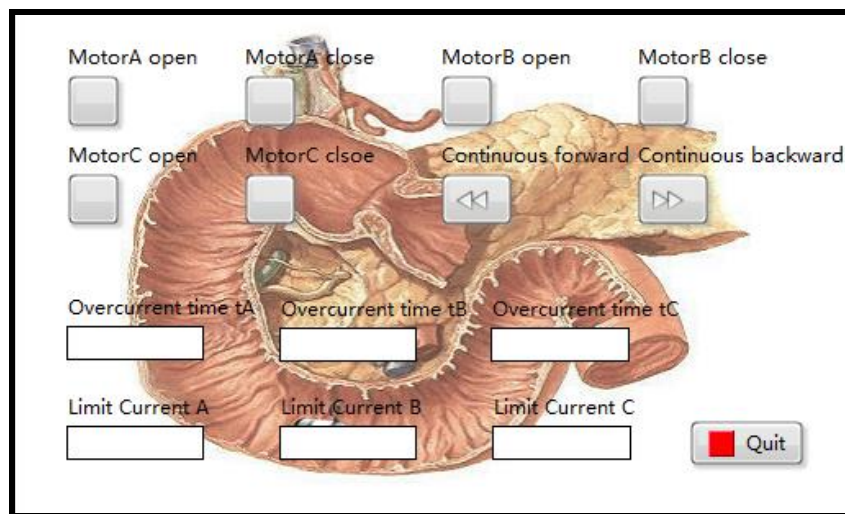


Figure 3.10: Operation Interface of the Integrated Interactive Interface

The programming structure adopted here is Queue Message Handler which avoids polling and possibility of losing the data. This structure is one of the Producer-Consumer Circle which contains multiple circles. It responds to user interface with processor-intensive applications, separating the user interface from processor intensive code. Only disadvantage of such structure is that it does not

integrate non-user interface events well which harms little in this case.

The core of such structure is demonstrated in Figure 3.11.

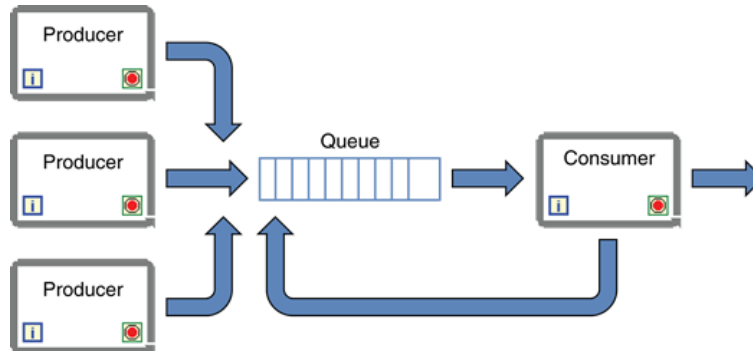


Figure 3.11: Schematic of the Queue Message Handler Structure

Figure 3.12 shows part of the programming block diagram. User event structure is used here so that the user events like clicking the buttons or close the front panel will be captured and recorded.

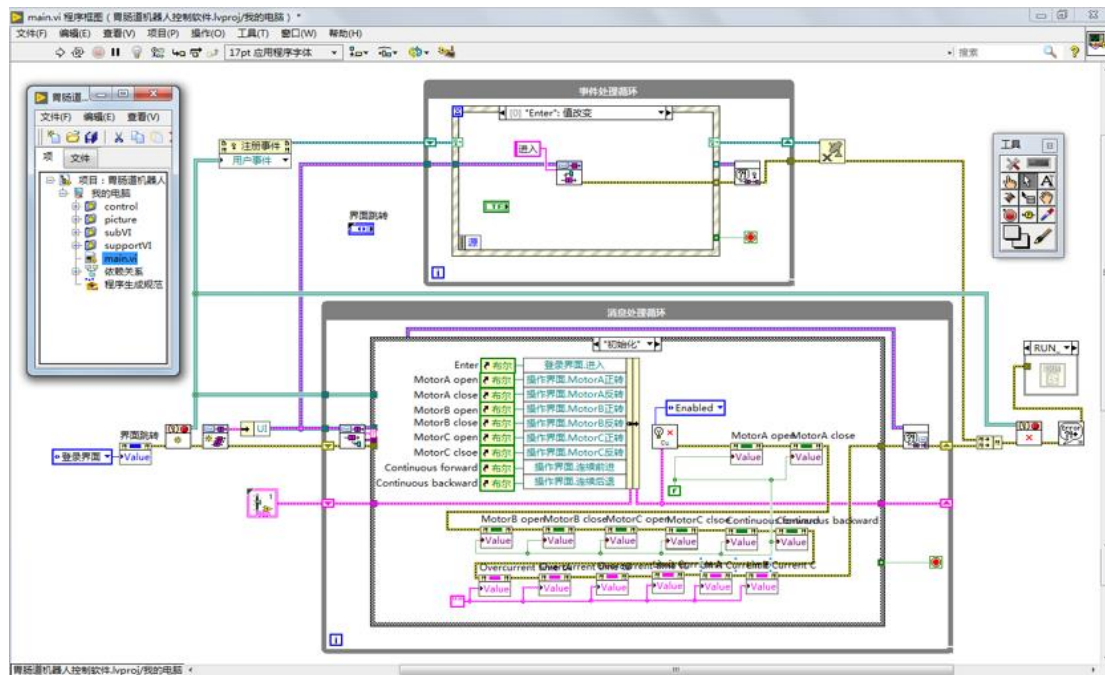


Figure 3.12: Programming Block Diagram

All data from the interface are bound into a cluster. The producer loop monitors every single command from the user interface, using event structure while the consumer loop deals with each state accordingly and process the data unbound from

the cluster. The virtual instrument (VI) illustrates an architecture which provides user a reliable way to queue multiple processes. Each process contains multiple states. The producer loop handles with the queueing of events. The consumer loop goes through the states of each process. The processed data is updated through shift registers. In this way, processes queued up can be easily in the order that the user selects.

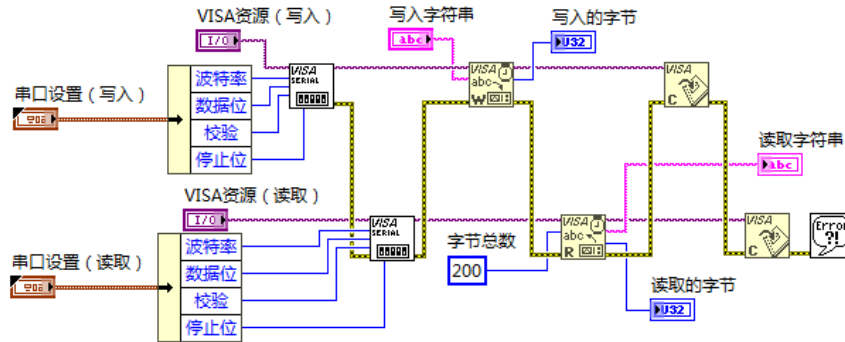


Figure 3.13: Serial Communication subVI

To realize serial communication, the Virtual Instrument Software Architecture, a standard for configuring, programming and troubleshooting instrumentation systems comprising Serial (RS232) interface, is installed. The serial write and read is realized in subVI with 9600 baud rate, 8 data bits, 1 stop bit, no parity bit and com port channel set. Figure 3.13 is the diagram of the subVI.

Chapter Four Experimental Verification and Result Analysis

Finishing the design of both the hardware and software of the wireless communication system of micro bionic robot, assembly coordination was done based on the robot assembled before to verify the effectiveness, rationality and reliability of the system.

The inchworm-like mechanism of the micro bionic robot is demonstrated in Figure 4.1, in which (a) is its model and (b) introduces its entity. The whole length of the robot is 45 mm and its diameter is 14 mm. With radial motion mechanism open, its diameter reaches 32 mm. With axial motion mechanism extended, the length reaches 54 mm. With alternate open and close of relevant motion mechanism, the robot can move actively in the intestine and the stomach.

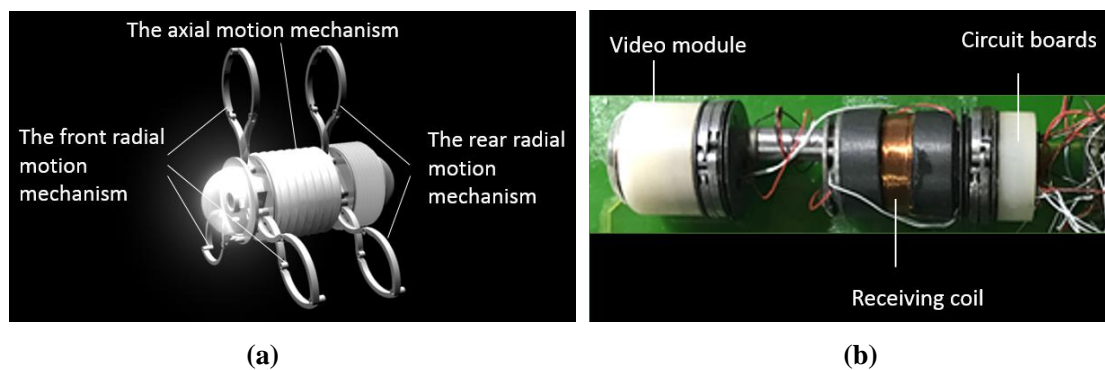


Figure 4.1: Prototype of the Robot

The whole robot is consisted of the mechanism, the wireless power transmission system, the wireless communication system, the user interface and the supporting subsystem.

Under DC power supply, the program can achieve 100% successful communication among the host computer, the external communication module and the internal communication module. Experiments were done to monitor the current. Figure 4.2 records the current monitoring process of the robot assembled with the Hall

sensors. The host computer sent commands to control the radial expansion and axial expansion mechanism to act repeatedly. The multimeter monitored the current and the EVEREST software displayed the current on the screen of the host computer. The maximum current of the radial motion mechanism and the axial motion mechanism was separately 0.066 A and 0.110 A. Even though there was no load, the friction force between the rears and other components caused the current rise of the radial motion mechanism. The axial current was nearly two time as large as the radial one because the friction force between the screws and nuts was larger than that of the radial mechanism. Meanwhile, the axial motion mechanism drove the radial motion mechanisms to move in the axial direction, which became its load. From the experiment which would be introduce in Chapter five, it could be known that the rotor lock current was over 0.3 A. So, both of the currents were below the threshold. So, it could be concluded that the Hall sensors functioned well. They effectively prevented the rotor lock which appeared at every beginning and end of the mechanism motion.

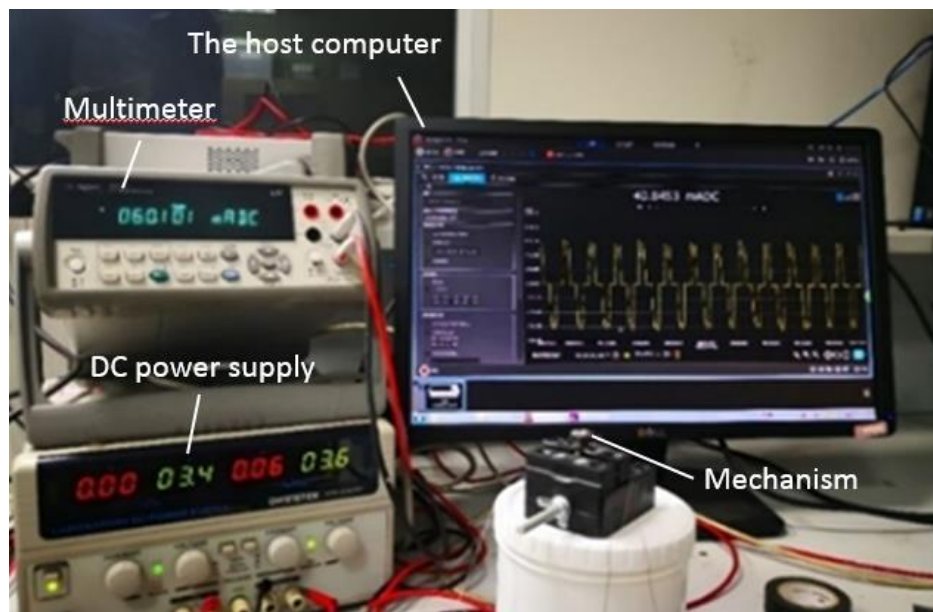


Figure 4.2: Current Monitoring Test System

Under wireless power supply, the system was also reliable. Then, a plastic tube was used to simulate the intestine as shown in Figure 4.3. The plastic tube limited the radial expansion, so the rotor lock happened before the Hall sensors work. It meant

that position module could not prevent rotor lock in all cases and this reflected in unstable wireless communication. What's more, other causes like unstable power supply, unknown friction could also lead to wireless communication failures. The Hall sensors could not be regarded as a panacea, they could only act as a safeguard.

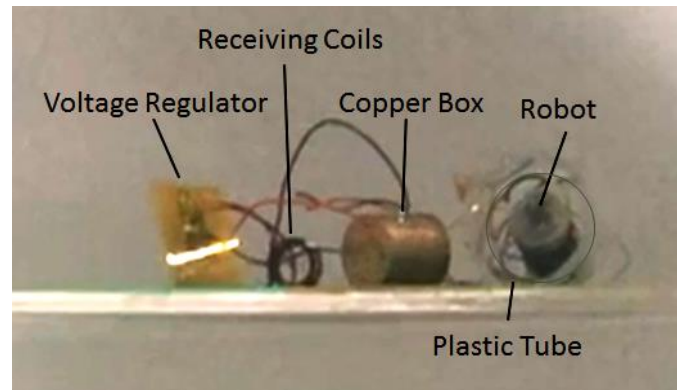


Figure 4.3: Stimulation of the Intestinal Environment

To take all circumstances into consideration, the position detection module was noted during further experiments and attempts for improvements.

The predicament at the very beginning was that the communication was erratic and irrational. Putting the whole robot system into the transmitting side of the wireless power transmission system, the communication occasionally achieved success. Sometimes the robot operated as expected while sometimes it was impervious to the commands. More over, even when inaugural communication succeeded, as long as rotor lock took place, the following communication attempts all end up in failures in any case. Only through shutting down and repowering up the transmitting side could the robot reset favorably. Under this circumstance, the receiving buffer had at least 16 bytes unchanged feedback, indicating that the command had been spent successfully. So, there must be something wrong with the internal communication module.

Since the robot system could operate faultlessly with DC power supply, a reasonable inference pointed out that the insufficient wireless power supply were the one to blame.

4.1 Transmitting Side Reconstruction

A premier conjecture was casted on the transmitting side of the wireless power transmission system.

As exhibited in Figure 4.4, the transmitting side is composed of a box and the transmitting Helmholtz coil which is a pair of double layer solenoids. Bottom 1, 2, 3 respectively control the on and off of the general power, the voltage and the current. The voltage knob controls the value of the voltage added to the Helmholtz coil while the tuning knob is connected to an adjustable inductance. The inductance was to be adjusted for resonance so that the power transmitted can reach its peak.

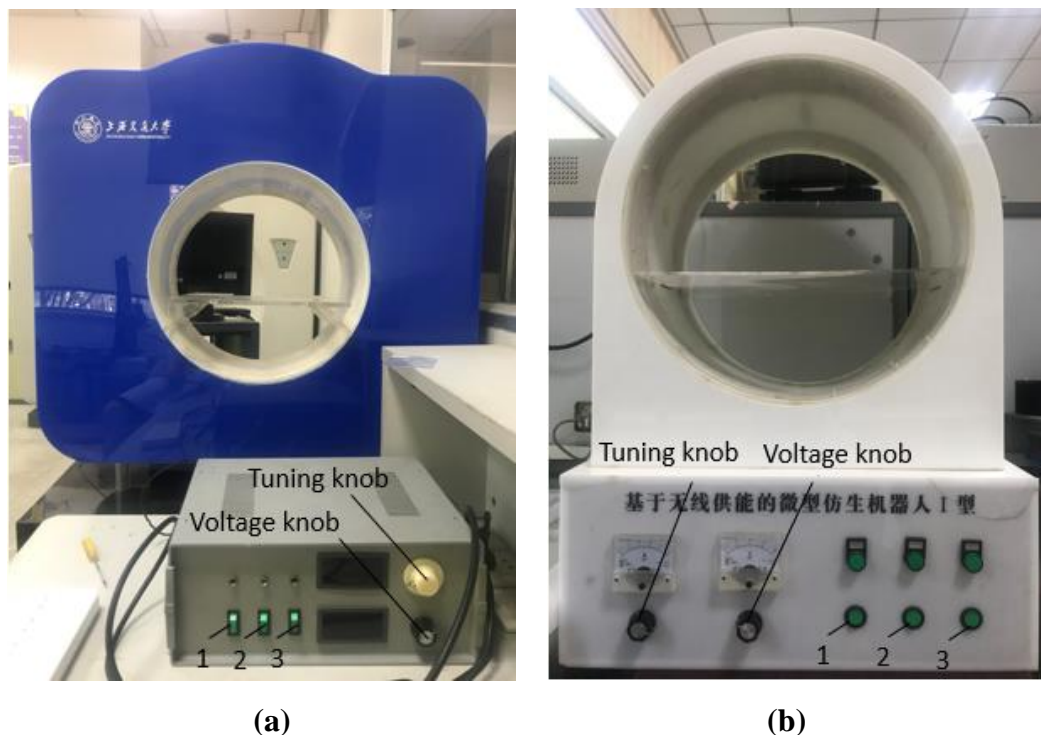


Figure 4.4: The Dubious (a) and Improved(b) transmitting box

Inside the bottom of box, there are a signal generator, a 3.3 V regulated power supply, a full-bridge inverter, an adjustable DC power supply as well as a vacuum capacitor and an adjustable inductance. The vacuum capacitor is used for resonance of

the pair of double layer solenoids. During the experiments, to get enough power for robot operation from the limited transmitting power, the transmitting voltage and current should be turned up. After numerous experiments, high voltage accelerated the ageing of the capacitor. During the experiments, when the voltage reaches about 13 V, current sound can be heard. Breakdown might even come along with capacitor discharge. Both of these two causes can lead to deficient power transmitted. To verify this conjecture, a new transmitting box was fabricated. Setting the transmitting conditions at 15 V and 3 A, the power sent from the new box could guarantee reliable inaugural communication. Thus, the conjecture was proved to be true and part of the problems were settled.

4.2 Energy Management Circuit

With the transmitting side reconstructed, the predicament turned to be that first command could be finished, however, the system failed to answer further commands after the rotor lock. Further analyzed, this might due to the inadequate voltage supply for the internal wireless communication submodule. When rotor lock happened, the current on the board rose in a sudden. As the power received could be regarded as stationary, the voltage would then be pulled down to less than 3.3 V suddenly. Thus, the chips in the internal module would enter crash or shutdown status, being unable to function well to offer durable communication.

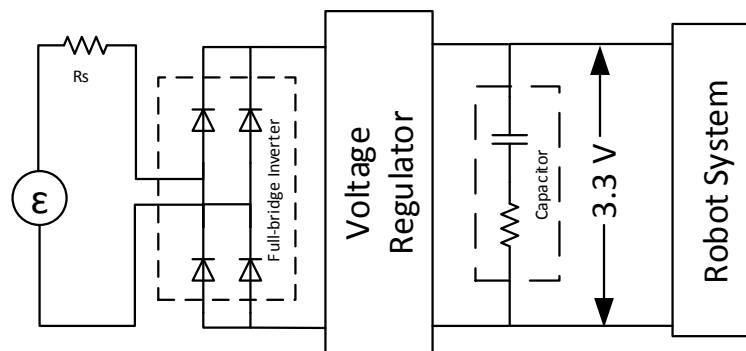


Figure 4.5: Overall Design of the Power Management Circuit

Energy management circuit were then taken into consideration to act as a buffer, in which decoupling capacitors played the key role as energy storage devices. They could make the output of the regulator uniform and reduce the load demand like a small rechargeable battery. The design of the energy management circuit is given in Figure 4.5.

Fitting after the voltage regulator module, the capacitor stores the electrical power and release when needed, in other words, when the voltage is suddenly pulled off. Generally speaking, decoupling capacitors are of μF capacitance. After investigation, super capacitors in Figure 4.6 were chosen.

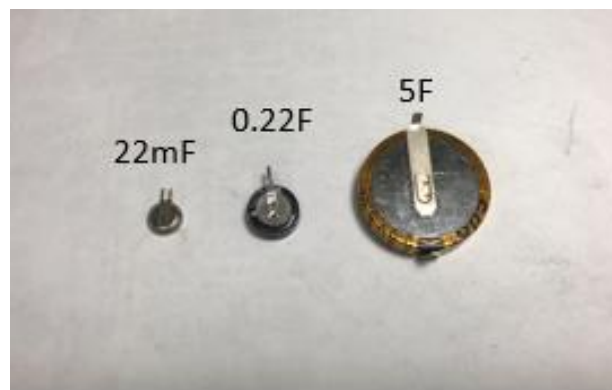


Figure 4.6: Super Capacitors

Super capacitor is a kind of electrochemical element for energy storage by polarized electrolyte. It has some similarities with traditional batteries and some characteristics of capacitors. It is a unique power source between these two concepts. Depending on the principle of double-layer and quasi-capacitance, electric energy can be stored without chemical reaction like other power resources, so it is reversible. Because of such reversibility, super capacitors can be recycled more than 100,000 times without memory effect.^[30] Its power density is five to ten times that of ordinary batteries. Cushioning effect was achieved through experimental corroboration. However, its shortcomings are ignorable. Low withstand voltage decreases system robustness. Large capacitance leads to long charging time, making the robot unresponsive. The most catastrophic dilemma is its magnetic sensitive susceptibility characteristic. Also, the data acquired from the experiments shows that super

capacitors can be greatly affected by magnetic field.

When adopting DC current supply, with 0.22 F super capacitor functioning as a buffer, the voltage over the capacitor was maintained soundly at 3.3 V. When using wireless power supply, with the transmitting coil under around 10 V, 1.2 A, the voltmeter witnessed a rise in the voltage over the capacitor to about 3.8 V. Then, other conditions were kept unchanged, varying only the position of the super capacitor. It turned out to be that the voltage over the capacitor was lowest in the center of the transmitting coil while higher near the edge of the transmitting coil. Taking the super capacitor out of the transmitting box, the voltage dropped to the expected 3.3 V. The inference was thus drawn that the magnetic field has massive disturbance towards the super capacitor. Furthermore, leaving other conditions untouched, the capacitance was adjusted to 0.02 F. This time, the reading of the voltmeter was still over 3.3 V, however, it halted at near 3.6 V, which was a little bit lower than that of the 0.22 F super capacitor. Another conclusion was then drawn that the larger the capacitance is, the more sensitive the capacitor is to the magnetic field.

The attempt of apply an energy management was proved by these experiments to be effective to some extent. However, it still calls for further improvement to solve the problems met and to offer reliable power guarantee.

4.3 Multi-coil Wireless Power Transmission

Aiming at improving transmission and system efficiency of the wireless power transmission system, an optimization scheme using a multi-coil structure composed of a transmitting coil, a receiving coil and a load coil was taken into practice. Previous studies have already proved the feasibility of multi-coil effectuating the transmission efficiency.^[31]

Figure 4.7 (a) is the diagrammatic sketch of the wireless power transmission system and Figure 4.7 (b) describes the system with a load coil affixed.

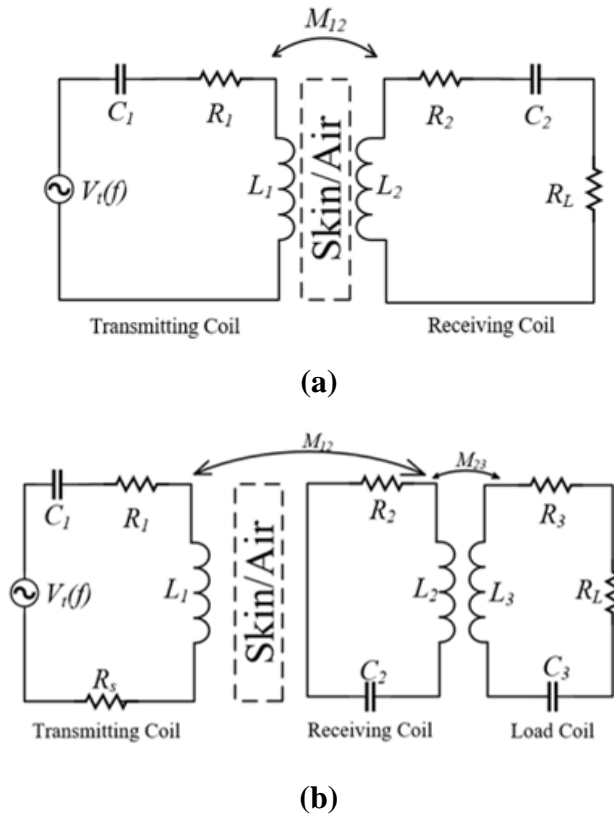


Figure 4.7: Diagrammatic Sketchs of the Wireless Power Transmission System

To put the theory into practice, experiments were done with load resistance changing from $30\ \Omega$ to $60\ \Omega$, which is the equivalent resistance range of the robot. The optimal resonance frequency is chosen to be 218 kHz and all these electrical specifications are measured by the impedance analyzer.

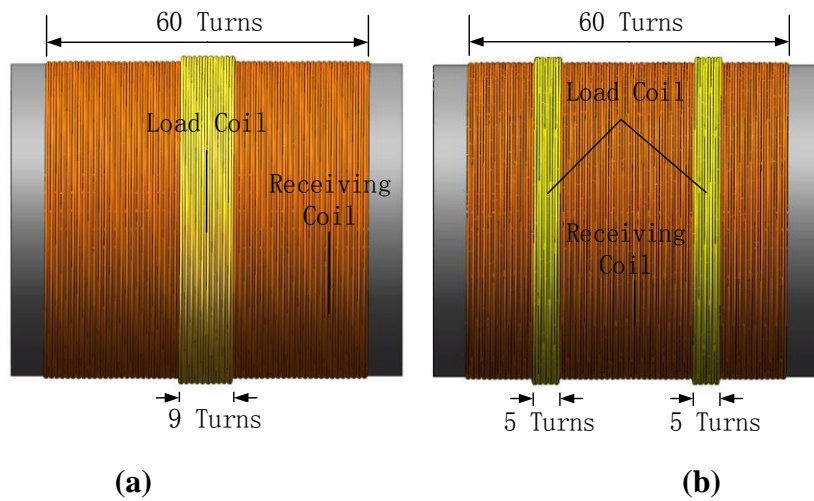


Figure 4.8: Coil modules

Meanwhile, inspired by the Helmholtz coil, the 10 turns load coil also took such structure, having 5 turns at each side. Figure 4.8 (a) describes the 9 turns load coil and Figure 4.8 (b) describes the 10 turns Helmholtz coil.

And Figure 4.9 demonstrates the result, energy efficiency improvement is satisfying. The multi-coil wireless power transmission system with 9 turns load coil achieved 4.32% transmission efficiency and the system with 10 turns Helmholtz structure provides the best rest of 6.45%.

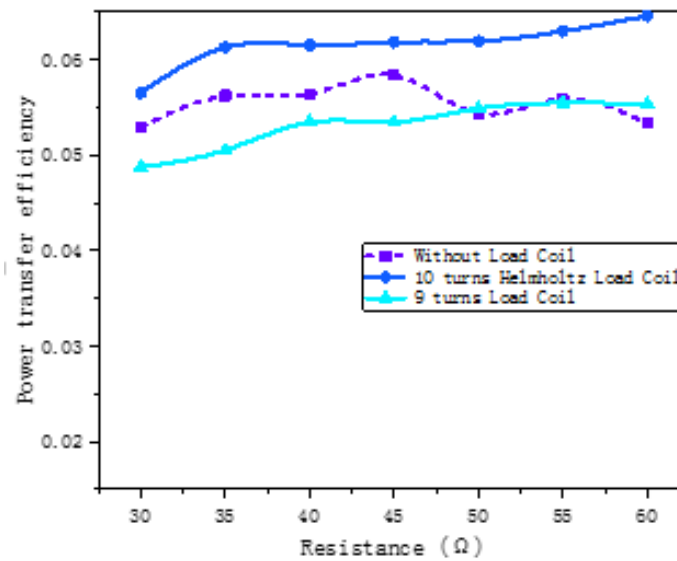


Figure 4.9: Power Transfer Efficiency Comparison

After optimizing the structure of the receiving part using multi-coil with a load coil affixed, with 13 V, 2.3 A power transmitted, the wireless communication can be ensured continuously. But the trouble was that the robot should be equipped with other supporting submodules like the LED and the video module to light up and show the in vivo environment in real application.

Table 4.1: Power Demand of the Robot Modules

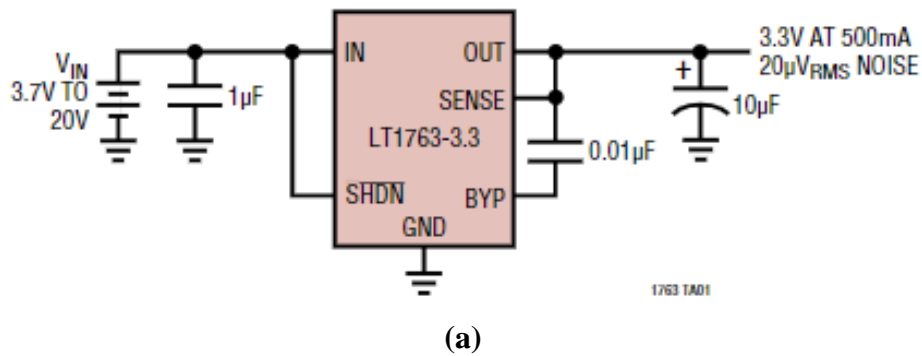
Module	Power demand (mW)	Running time ratio
Video	20+12	100%
LED	4×10	100%
Control	40	100%
Communication	40	40-60%
Mechanism	400	10-60%

The whole power demand of the robotic modules designed are listed in Table 4.1.

So, the whole energy demand is roughly calculated about 600 mW. After equipping the LED and the video module, the subsequent communication unfortunately ended up in failure. Result confirmed that the received power improvement offered via new coil structure was not enough for additional 72 mW power demand.

4.4 Voltage Regulator Chip Reselection

Except for increasing the power transmitted, offering a power buffer, improving the transmission efficiency, lowering down power consumption was also tried. When doing the experiments, the voltage regulator was always found excessively hot.



3.3V_{OUT} from 5V_{IN} to 40V_{IN} Step-Down Converter

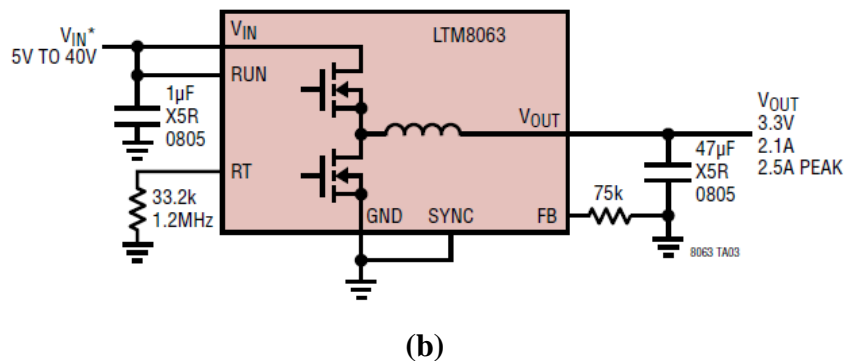


Figure 4.10: LT1763 Voltage Regulator (a) and LTM8063 Voltage Regulator (b)

The reason was inferred to be that when the current flowing through the motor

raised in a sudden because of the rotor lock, the current output by the voltage regulator could not satisfy the need any more. The experimental environment was settled with $20\ \Omega$ load resistance, 14 V, 2.5 A transmitting power. Measuring after a single rectifier module, the voltage was 6.7 V and the power calculated 2.24 W. Applying the voltage regulator after the rectifier module, the power for the $20\ \Omega$ load resistance was 0.5445 W. However, operating at a current over its maximum current range, the output voltage could not be ideally regulated and was extremely unstable.

The original voltage regulator chip is the micro power, low noise LT1763 introduced in Figure 4.10 (a). It can be known from the datasheet that its maximum output voltage is 500 mA and the dropout voltage at this current value is 300 mV. Providing its maximum output current, the voltage regulator gets over hot and can not function normally. Extra power spent on heating means relatively low power efficiency.

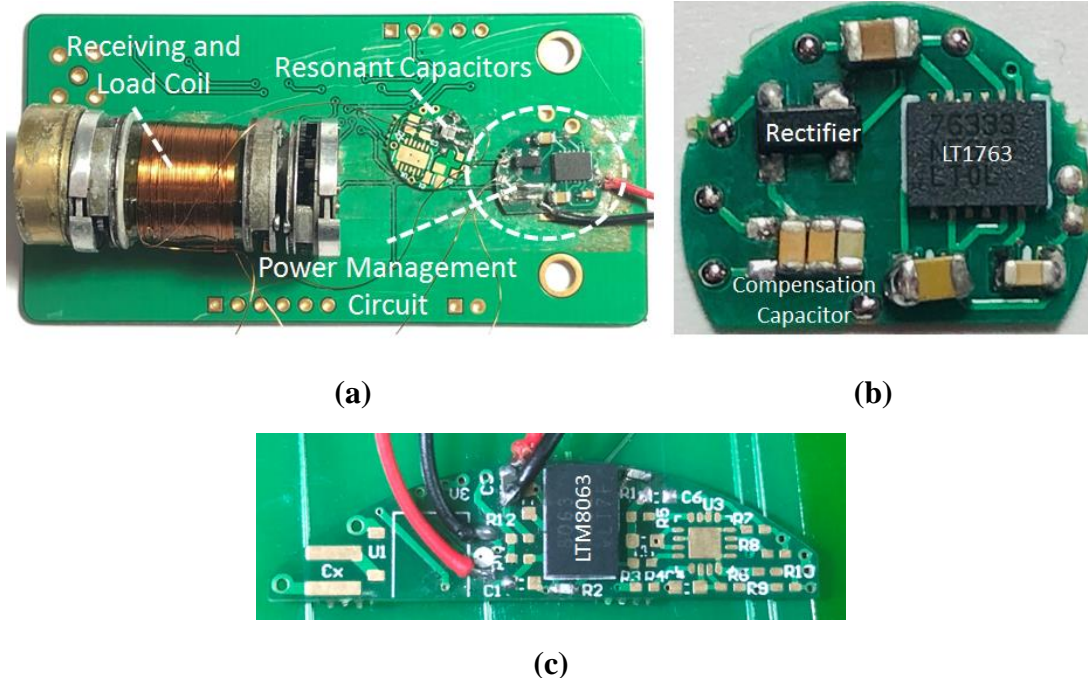


Figure 4.11: Voltage Regulator Test

So, another voltage regulator which can afford larger current with larger maximum output current was supposed to take its place. Then, LTM8063 in Figure

4.10 (b) was chosen after investigation. Operating over an input voltage range of 3.2 V to 40 V, the LTM8063 supports an output range of 0.8 V to 15 V. From its datasheet, it can afford typically 2 A current as maximum. Providing a 3.3 V output, its power efficiency is recorded to be around 85%.

Experiments adopting the LTM8063 voltage regulator perfectly met the expectation to offer stable voltage output without going too hot. Figure 4.11 (a) shows the power receiver and the power management circuit which is magnified in Figure 4.11 (b). Figure 4.11 (c) exhibits the LTM8063.

4.5 Programming Optimization

With all these efforts done to ameliorate the transmission efficiency, the fundamental stable communication was still left unguaranteed. As analyzed previously, the communication failure was due to deficient voltage supply received in the internal wireless communication submodule, pulled down because of the current surge brought by rotor lock. The sudden drop of the voltage made the chips on the internal board enter the brown-out state which was similar to computer crash.

Since the current detection module was designed to prevent rotor lock motor through monitoring the current. The first attempt considered setting the threshold of the current lower to make full use of the current detection module so that the voltage decrease would not be so large as to affect the voltage supply of the internal wireless communication submodule. This method works in theory. But when taken into practice, since each motor has its own characteristic, different motor should enjoys different threshold value. The critical point can only be detected through numerous tests. So, this method has no practical value because of endless effort it calls for.

The datasheet of PIC24F16KA102 introduces that this device implements a Brown-out Reset (BOR) circuit, which provides the user several configuration and power-saving options. The BOR is controlled by the BORV<1:0> and BOREN<1:0>

Configuration bits. The BOR threshold is set by BORV<1:0> bits. If BOR is enabled (any values of BOREN<1:0> other than '00'), and drop of voltage supply below the set threshold point will reset the device. The chip will not leave BOR state until the voltage supply climbs back above the threshold. Meanwhile, power-up timer is set enabled in configuration bits. The timer will be invoked as soon as the voltage rises above the threshold. Then, it will keep the chip staying at the reset state for an extra time delay if the voltage drops below the threshold again while the power-up timer is running. The timer is 64 ms when enabled. Each time when the MCU goes back into a BOR, the timer will be initialized. The software enabled BOR was not used here as this function was in need throughout the whole process. The BOR threshold was chosen 2 V and the reason will be mentioned below.

For the chip SI4455, however, after carefully reading its datasheet, there are no BOR state. Five primary states of the SI4455 are shutdown, standby, SPI active, ready and power on reset (POR) introduced in Figure 4.12. Except for the shutdown state, all other states are controlled using API commands.

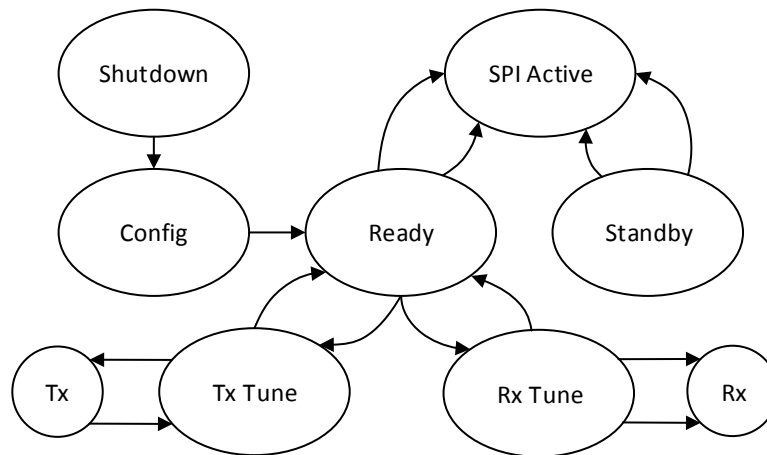
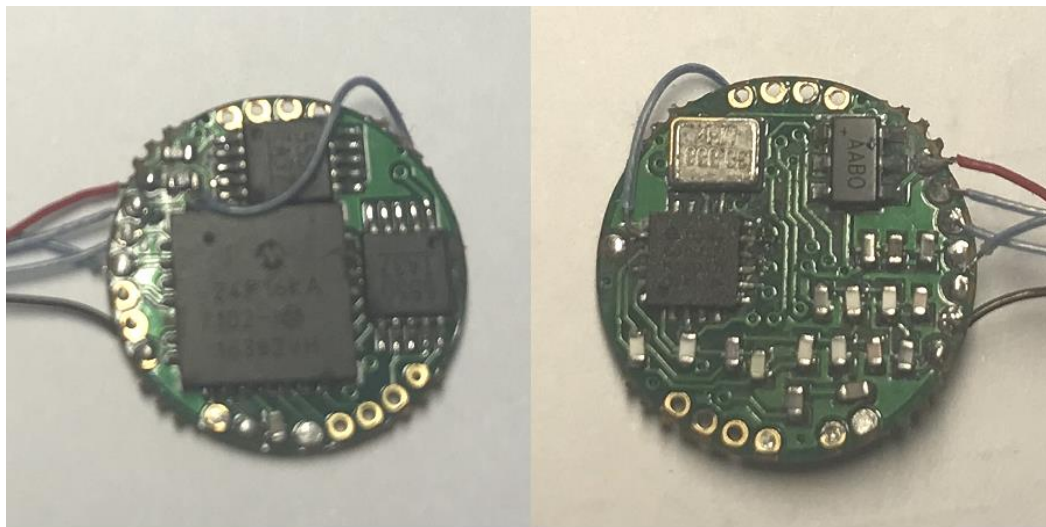


Figure 4.12: State Machine Diagram of SI4455

In the shutdown state, all register contents are lost and there is no SPI access. To exit this mode, SDN should be driven low. At the very beginning, the SDN port was directly connected to the ground as shutdown state was thought to have no use since wireless communication were supposed to work continuously throughout the whole diagnosis and treatment process. But the predicament brought by insufficient pulled

down power supply was its crash, entering the shutdown state. According to the datasheet, in order to exit the shutdown state, after driving the SDN low, the device will then initiate a POR along with internal calibrations. A POR sequence is used to boot the device up from a fully off or shutdown state. Once this POR period is complete, the POWER_UP command is required to initialize the radio and the configuration can then be loaded into the device. The SDN pin must be held high for at least 10 μ s before driving it low again to insure the POR can be executed correctly. The shutdown state and the POR seems to be the only way to reset this part. If POR timing and voltage requirements cannot be met as what happened in this case, the SDN should be controlled using the host processor rather than tying it straightly to the ground on the board. To confirm this deduction, the SDN pin was connected to the PIC by a wire welded presented in Figure 4.13.



(a) (b)

Figure 4.13: Test Board Connecting the SDN pin to PIC

Meanwhile, the programming was rewritten to match this change. Figure 4.14 displays the improved flowchart of the internal wireless communication submodule with BOR reset of the internal communication submodule completed. It should be pointed out that the shutdown and power on of SI4455 is actually included in the main function of the MCU. It means that the realized BOR of SI4455 is fulfilled with the

BOR of the MCU. What's more, the BOR does not simply solve the accidents caused by rotor lock overcurrent, any other unexpected events like magnetic field change, unordinary movement pulling the power supply lower than the set threshold can all be solved through the BOR of the internal communication submodule.

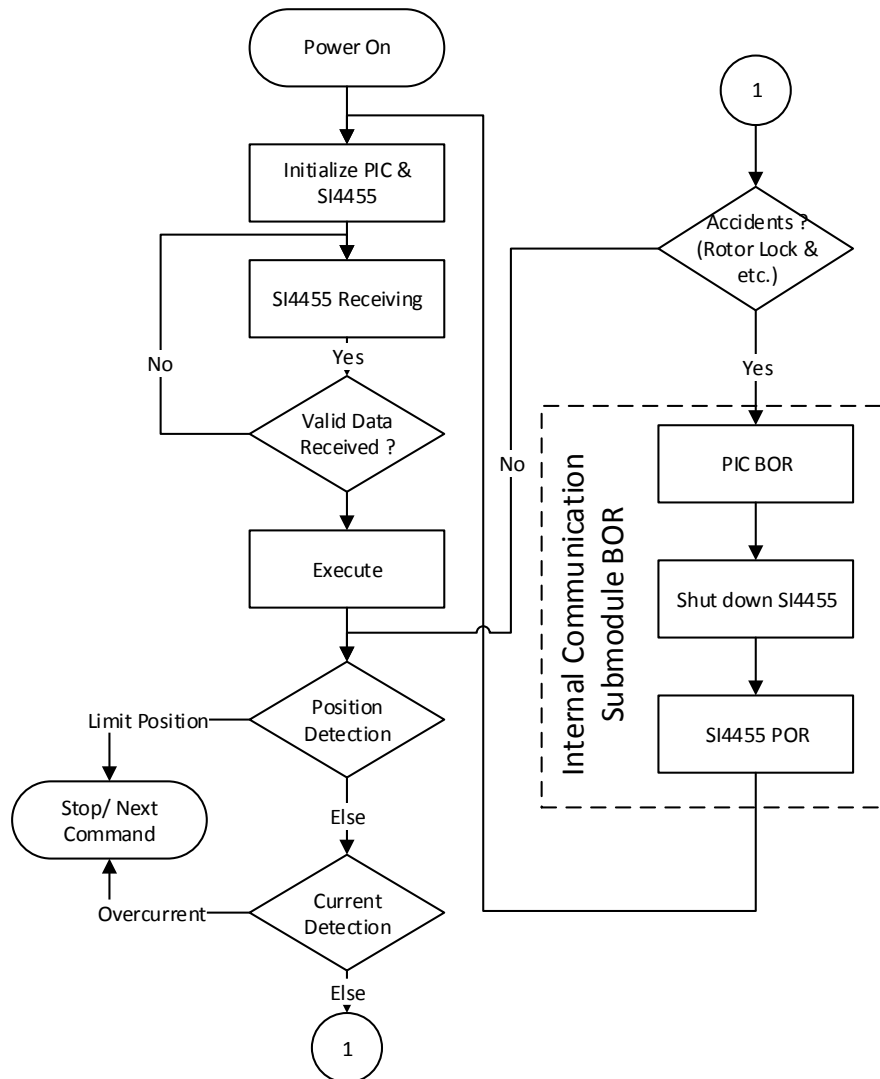


Figure 4.14: Improved Overall Flowchart of the Internal Wireless Communication Submodule

Except for the command added in the programming, the configuration bits should also be updated to catch up with the new program. To avoid circumstance that the PIC sends command while the SI4455 has already shut down, the threshold of BOR voltage should be synchronized for both of them. The value was chosen according to the supply voltage of SI4455 covers from 1.8 V to 3.6 V. Since the quality of the chips is not elaborately pledged, 2 V became the final choice.

Using this optimized software, sustainable and reliable wireless communication could finally be realized with 100% success even when equipped with those supporting modules. What's more, the copper box used for shielding electromagnetic interference which mattered previously was not a necessity any longer.

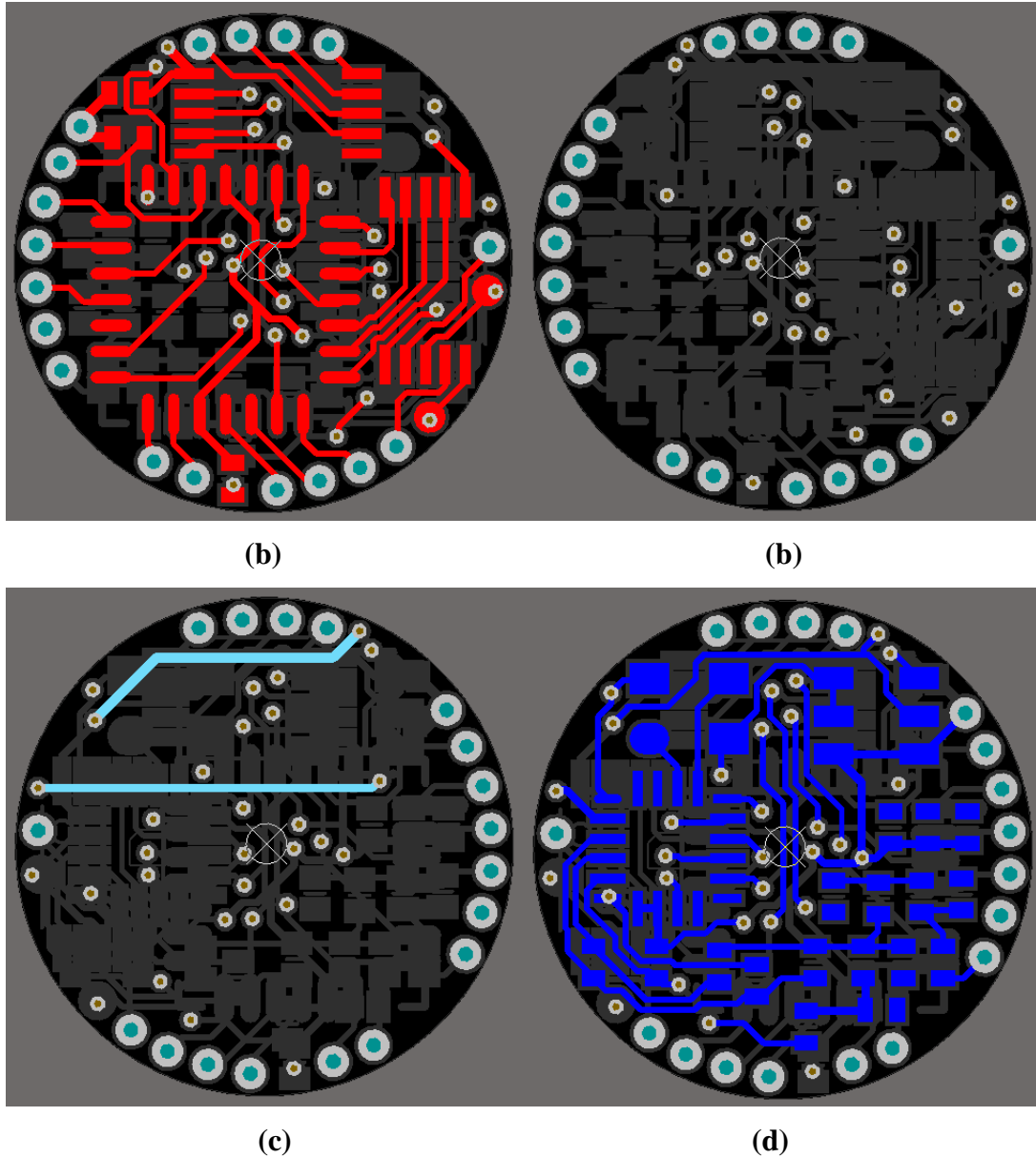


Figure 4.15: PCB Board Design of the Internal Wireless Communication Module

Thus, this experiment gained a success. Then, the PCB board was redesigned for implementation. For the reason that there was strict demand on the size of the board

of the internal module and there was literally no place to connect SDN pin and the pin of the MCU, the internal wireless communication PCB board was designed to be a four-layer board as shown in Figure 4.15. The ground layer also acted the shield function. In this figure, (a), (b), (c), (d) presents separately its top layer, ground layer, VCC layer and bottom layer.

Since the steadiness of the wireless communication system is ensured, another experiment was done to figure out the influence of various communication distances and the helical antenna.

Table 4.2: Success Rate Experiment of the Wireless Communication

Distance (m)	Receptions with antenna	Receptions without antenna
5	50/50/50	50/50/50
10	50/50/50	49/50/48
15	50/50/50	48/49/47
20	50/50/49	49/37/41
25	47/48/47	35/32/37
30	43/42/42	28/22/28

The distance was changed from 5 m to 30 m, 5 m as an interval, according to the 20 m theoretical communication distance of SI4455. Both the transmitting side and the receiving side was kept at the height of 1 m. The medium is air. At each testing point, 3 groups of tests were done to avoid random errors. Each group included 50 communication attempts between the host computer and the robot system. 36 groups of data were collected in total with 1800 communication attempts casted. Detailed information is presented in Table 4.2. Figure 4.16 displays the success rate trend.

The antenna was proved to have large influence on the wireless communication result. It helped improving both the success rate of the wireless communication module as well as prolonging the effective communication distance. The wireless communication achieved complete success regardless of the antenna when the

distance was less than 5 m. Since the communication distance is usually under 5 m in application, the wireless communication system has already met the initial expectation with 100% communication success proved. The over 90% success rate under the distance less than 15 m without antenna was also acceptable. With the antenna assembled, the effective communication distance increased to 25 m. To provide stable communication and expand the communication range, antenna was assembled onto the robot system.

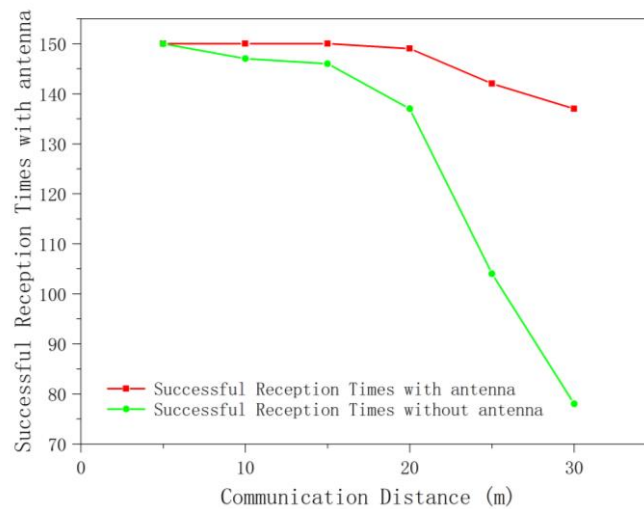


Figure 4.16: Success Rate Trend

Previously with the biggest problem left unsolved, the position detection submodule was noted for the convenience of debugging. After the problem being ironed out, the program whose detailed design has already been introduced in Chapter Four was expected to fulfill the function of position detection submodule using the Hall sensors. Putting the robot system into the wireless power transmitting box, the front motion mechanism could not close properly, characterized by constant trembling. Sending other commands the axial and rear mechanism worked well. So, it was suspected that the Hall element settled in the front was not at its right place. Adjusting the Hall sensors meant the dismemberment of the whole robot mechanism. So, the final decision was made to invalidate the front position detection submodule which was realized through changing the corresponding bits of the control words sent. Thus, the movement of the whole robot system could meet expectation.

With all these attempts done, it could be figured out that the key problem lies in the lack of BOR of SI4455 and the former failures could all be explained as followed.

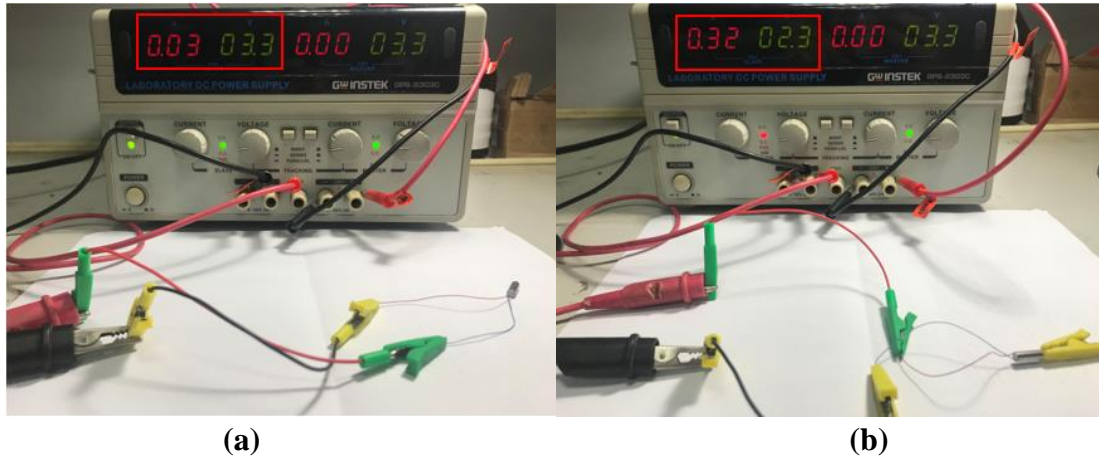


Figure 4.17: Working Current (a) and the Rotor Lock Current (b)

During the process of robot movement, each time when the robot comes to the end of its single movement, the rotor lock occurs. Then, the current increases rapidly. The actual rotor lock current was measured to be about 0.32 A shown in Figure 4.17. The working current of the rotor was 0.03 A while the rotor lock current dropped to 2.3 V. It was worth mentioning that once in a case in which the pin of current-sense amplifier was validly welded, the rotor lock current was measured 0.45 A. This demonstrated the influence brought by robot lock was magnificent.

From all those written above, there is no doubt that power supply is of great importance to the micro bionic robot system. Any tiny power improvement can make a difference. Previous works all focus on ensuring the power transmitted and improving the transmission efficiency. Saving the power consumption can also be a nice point of view. Taking the elements on board into consideration, there are two chips that owns a power saving mode. One is the PIC24F16KA102 and the other is the SI4455.

The MCU incorporates a range of features that can significantly reduce power consumption during operation. Key items include on-the-fly clock switching, doze mode operation and instruction-based power-saving modes which are idle mode, sleep mode and the deep sleep mode. Fluctuating clock speed and invoking one of the

power-saving modes are the general strategy for reducing unnecessary power consumption. Under the circumstance where it is vital for a device to maintain uninterrupted synchronous communication, even while it is dealing with nothing. Communication faults will be introduced by reducing system clock and communications may be stopped completely adopting a power-saving mode. Doze mode is a simple and effective way to save power with the devices executing code without obstacles. In such mode, the system clock still operate from the same source at the same speed. Peripheral modules continue to be clocked at the unchanged rate. The only thing differed is the lower down CPU clock speed. The two clocks are synchronized, allowing the peripherals to access the special function registers. Furthermore, the peripheral modules can be selectively disabled to eliminate their power consumption. However, as there seldom exists any break for the MCU and how much power can be saved can not be estimated, whether this attempt can get any achievement is uncertain.

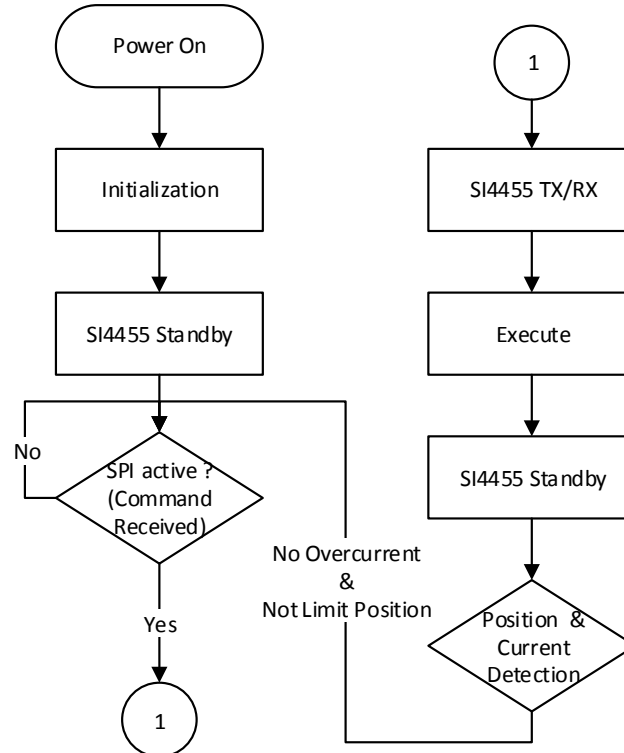


Figure 4.18: Implementing the Standby State of SI4455

For SI4455, the specific situation is different. During the experiment, when the

SI4455 was not shutdown and the motor was running, the current read from the DC current supply was 0.06 A. However, when setting the SDN to 1, the current dropped to 0.04 A. This indicates that nearly 66 mW power may be saved if the SI4455 could be shutdown. But if the SI4455 is shutdown, data transmission may be interfered. The standby state retains all register values and enjoys similar current consumption to the shutdown state. The response time of shutdown and standby state is separately 30 ms and 500 μ s and the current difference is only 20 nA. It should be pointed out that after the SPI event which transition the chip to the SPI active state, the host needs to re-command it back to the standby mode. Based on comprehensive consideration, making use of the standby state may be a better choice. Primary design is displayed in Figure 4.18.

Chapter Five Conclusions and Future Works

5.1 Conclusions

To conclude, the research progress can be separated into two stages. During the former stage, the research focused on the design of both the hardware and software of the wireless communication module with assembled Hall sensors. Successful experiment resulted under both DC and wireless power supply proved the feasibility of the design. To prove the practicability of the design, experiments were done onto the assembled robot system in a plastic tube to stimulate its movement in real intestine. Failures suggested the instability and defect of the design.

The later stage aimed to figure out the crux and solve the problems making the communication unstable. Experiments were designed and carried out from various aspects to confirm the suspects.

The whole power supply of the system is around 600 mW, when motor start or rotor lock, the obviously increasing current will lead to a sharp drop of voltage. The calculated value of voltage was supposed to be at least under 1.875 V. Meanwhile, the experiments show that when the voltage drops below 2 V, the wireless communication of the internal communication submodule fails. Therefore, the communication system is unstable during the stage of motor start or rotor lock.

The first attempt which improved the output of power transmitter to ensure the power transmitted so that the first communication after powering up could be guaranteed in any condition. The power management circuit introduced the use of super capacitor as a buffer, to stabilize the power supply for the robot rather than easily affected. Experiments proved its appreciable buffer ability, however, it could be affected by the magnetic field to a great extent. The voltage could not be stabilized to

the ideal value which meant it was not a proper choice in this case. Further experiments shall be made to give explanations and make improvements. The multi-coil structure which imported an intermediate coil in the receiver part improved the transition efficiency to a relatively greater extent. After improving the transmitter coil and introducing the multi-coil structure, communication success rate was greatly improved. Meanwhile, since the maximum output current of the new voltage regulator LTM8063 was considerably larger, the voltage regulator consumed less power and thus saved received power for the robot. Under the condition without supporting modules, the wireless communication achieved full success. However, the fact was that the consequence brought by motor lock was serious and the power demand of the supporting modules could not be ignored. Even with all these improvements, the communication failure could not be totally avoided with supporting modules equipped. The program optimization was regarded as a useful method to solve this problem rather than finding methods to prevent rotor lock. And perfecting the program in logic improved the system robustness. When the stuck happened, by applying the newly designed program, the system could recover itself.

Thus, the reliability and sustainability of wireless communication can be guaranteed.

5.2 Future Works

Based on the current achievement and shortcomings, future works are expected from the following aspects.

A. Video module

As introduced previously in Chapter three, video module is an indispensable part of the whole robot system. Without a reliable, power-saving, video module with high resolution, the robot will be working nonsense. After completing all other functions,

the video module should be added onto the robot system. Except for achieving reliable video acquisition and transition, the following image processing and video processing should be taken seriously. Numerous researches have already been done in related areas and further achievements are expected.

B. Orientation Control

For now, the transmitting coil and the receiving coil are both one-dimensional. The change of the angle between the transmitting coil and the receiving coil leads to a drop in the power received. Without sufficient power supply, it is impossible for the robot to execute any command. Except for trying three-dimensional coil either for transmitting or receiving which is hard to realize, an orientation-based control system seems to be more practical with numerous advantages. By monitoring the location of the robot in the human body, especially its orientation, the orientation and position of the transmitting coil can change synchronously, keeping the two central axis coincided. Thus, the transmission efficiency can be ensured.

Moreover, the intestine of the human body is not straight forward. Accurate control of the robot movement should be established. The orientation system helps to obtain the feedback of close loop control. Design on control flexibility should be taken into consideration on the base of that. Thus, the security of the system can also be ensured, preventing robot caused intestinal perforation.

C. Safety Design

Working in the stomach and intestine inside the human body, the safety stand surely the first place. Robot-assisted surgery for the intestine has undoubtedly brought certain benefits along with associated complications. According to previous investigations, the incidence of therapeutic colonoscopy intestinal perforation was 0.073% to 2.14% and that of diagnostic intestinal perforation was 0.03% to 0.65%. The perforation of sigmoid colon and the transitional part between sigmoid colon and descending colon happened frequently and accounted for 82.1% while that of rectum

and the transitional part between rectum and sigmoid colon covered 77.7%., showing that perforation was easy to take place in the corner of the intestinal, namely the hardest part for the robot to pass through.^[32] Taking only gastrointestinal injuries into account, the incidence of bowel injury is about 1.3 per 1000 cases.^[33] These all indicate the fragility of the intestine.

There are two main causes of intestinal perforation. One is the the injuries to the intestinal wall caused by instruments. This often happens when the endoscope is blindly inserted without full acknowledgement of the intestinal environment. Then, direct damage is casted on the intestine by the end of the endoscope. The other cause is unaffordable axial pressure. When the endoscopy stretches the intestine to a certain extent, its wall will be perforated. Especially under the condition with colonic diverticulum, ulcer or intestinal adhesion, the risk of perforation increases.

To avoid such tragedies, two schemes may be valuable.

First scheme suggests pressure sensors monitoring the pressure at the ends of the motion mechanisms. As long as the largest pressure is under the safety threshold, injuries will be definitely prevented. Eddy current sensors, Inductive sensors and Hall sensors are all magnetic sensitive and are put out of consideration. Capacitive ones are too large in size with poor linearity and its circuit is complicate. Piezoelectric ones and piezoresistive ones seem to fit.

Second idea is to invent a brand new mechanism. Paddle type robot and spherical robot with multi micro feet may be practical choices.

REFERENCE

- [1]. Organization, W.H. *World Health Statistics 2018*. Global Health Observatory (GHO) data 2018; Available from: https://www.who.int/gho/publications/world_health_statistics/en/.
- [2]. Choi, K.S., et al., *Effect of endoscopy screening on stage at gastric cancer diagnosis: results of the National Cancer Screening Programme in Korea*. British Journal of Cancer, 2015. **112**(3): p. 608-612.
- [3]. 陈爱兰 and 樊宇芳, 消化道癌的社区筛查及早期诊断的研究进展. 中国药物与临床, 2018(1): p. 55-56.
- [4]. Habrgama, A. and J.D. Wayne, *Complications and hazards of gastrointestinal endoscopy*. World Journal of Surgery, 1989. **13**(2): p. 193-201.
- [5]. Reiertsen, O., et al., *Complications of fiberoptic gastrointestinal endoscopy--five years' experience in a central hospital*. Endoscopy, 2008. **19**(01): p. 1-6.
- [6]. 张巍 and 邓明明, *SELDI 蛋白质芯片技术在结直肠癌临床诊断中的应用及发展前景*. 西南医科大学学报, 2009. **32**(2): p. 183-185.
- [7]. 何勇 and 郑艳, 消化内镜技术发展现状及其未来应用趋势. 现代养生, 2015(8): p. 287-287.
- [8]. 李兆申, *中国消化内镜现状及展望*. 解放军医学杂志, 2010. **35**(1): p. 5-8.
- [9]. Gao, J. and G. Yan, *Locomotion Analysis of an Inchworm-like Capsule Robot in the Intestinal Tract*.
- [10]. Nakamura, T. and A. Terano, *Capsule endoscopy: past, present, and future*. Journal of Gastroenterology, 2008. **43**(2): p. 93-99.
- [11]. Li, Z., et al., *The Current Main Types of Capsule Endoscopy*. 2014.
- [12]. Amy, W., et al., *Wireless capsule endoscopy*. 2008. **14**(13): p. 717-719.
- [13]. Eliakim, R., ., et al., *Prospective multicenter performance evaluation of the second-generation colon capsule compared with colonoscopy*. 2009. **41**(12): p. 1026-1031.
- [14]. Leighton, J.A. and S.F. Pasha, *Capsule and Small Bowel Endoscopy*. 2016.
- [15]. Rasouli, M., et al. *Wireless capsule endoscopes for enhanced diagnostic inspection of gastrointestinal tract*. in *Robotics Automation & Mechatronics*. 2010.
- [16]. Sliker, L.J., et al., *Surgical evaluation of a novel tethered robotic capsule endoscope using micro-patterned treads*. 2012. **26**(10): p. 2862-2869.
- [17]. Lee, C., et al., *Active Locomotive Intestinal Capsule Endoscope (ALICE) System: A Prospective Feasibility Study*. IEEE/ASME Transactions on Mechatronics, 2015. **20**(5): p. 1-8.
- [18]. 张永顺 and 杨慧远, 磁场与视觉共融的多模态胶囊机器人人机交互控制. 机器人 Robot, 2018. **40**(1): p. 72-80.

- [19]. Guo, J.B., Zihong & Guo, Shuxiang & Fu, Qiang, *Design of A Novel Drug-delivery Module for Active Locomotive Intestinal Capsule Endoscopy*. 2018(1633-1638. 10.1109/ICMA.2018.8484692.).
- [20]. Zhou, J., et al. *Overview of Medical Robot Technology Development*. in 第37届中国控制会议论文集 (D) . 2018.
- [21]. WIKIPEDIA——Wireless Communication.
- [22]. 陈胜, 近距离无线通讯技术发展分析. 电子技术与软件工程, 2015(3): p. 49-49.
- [23]. 郭亮, 基于 433MHz 的微功率无线通信系统的设计与应用. 2016, 湖南大学.
- [24]. 吴恒 and 周涛涛, 体内微型软体机器人的无线通信系统设计研究 机械与电子 Machinery & Electronics, 2013(12): p. 67-69.
- [25]. 刘冬, 汪彬, and 张建勋, 机器人控制系统数据采集和通讯方法的实现. 自动化与仪表 AUTOMATION & INSTRUMENTATION, 2010. **25**(10): p. 5-7,19.
- [26]. 李亮波, 刘继忠, and 张.J. 微计算机信息, 胶囊机器人无线控制系统设计. 2010. **26**(11): p. 157-158.
- [27]. 刘波, et al., 基于nRF24LE1 的无线胶囊内窥镜医疗机器人. 华中科技大学学报 (自然科学版) , 2013. **41**(s1): p. 293-296.
- [28]. Bhardwaj, et al., *Wireless data acquisition for industrial, scientific and medical purposes*. 2017.
- [29]. 植入式医疗设备无线能量传输系统电磁环境下的人体安全性研究. 2014, 中国海洋大学.
- [30]. 胡毅, et al., 超级电容器的应用与发展. 2008. **9**(1): p. 19-22.
- [31]. Li, Z., et al., *Transfer Efficiency Analysis of Magnetic Resonance Wireless Power Transfer with Multiple Intermediate Resonant Coils*. Transactions of China Electrotechnical Society, 2013. **2**(6): p. 1143-1152.
- [32]. 黄文峰, et al., 肠镜检查并发肠穿孔 42 例报告. 中国内镜杂志, 2000. **6**(5): p. 80.
- [33]. Velilla, G., et al., *Visceral and gastrointestinal complications in robotic urologic surgery*. Actas Urologicas Espanolas, 2018. **42**(2).

ACHIEVEMENTS DURING THE STUDY FOR BACHELOR'S DEGREE

- [1] Yicun Meng, Guozheng Yan, Ding Han, Pingping Jiang, Wei Wang, Yiyun Wang, *Optimization and Analysis of a New Type Receiving Part in Wireless Power Transfer System Applied in Gastrointestinal Robot* (submitted)
- [2] 温桢妮, 颜国正, 王志武, 薛蓉蓉, 王艺芸, *肠道机器人三维接收线圈的设计与优化* (submitted)
- [3] Shuai Kuang, Guozheng Yan, Zhiwu Wang, Yiyun Wang, *An Efficient Analytical Model on Mutual Inductance for Wireless Capsule Endoscopy* (to be submitted)
- [4] 颜国正, 孟一村, 韩玓, 姜萍萍, 王志武, 汪炜, 陈范吉, 温桢妮, 王艺芸, *亥姆霍兹线圈式的三线圈无线供能系统* (applied for national invention patent of China)

ACKNOWLEDGEMENTS

I still remember the first time when I knocked at Professor Yan's door. It was an early autumn, the path to our school buildings started to be embellished by fallen leaves of red and gold while the sunshine was no longer as dazzling and vital as it was in midsummer. At that time, I had totally no idea of my graduation project at all. The only thing I had was the eager to learn for micro bionic robots. Nearly one year has passed, I have now a general cognition of the micro robot system for noninvasive gastrointestinal diagnosis. This semester spent in the laboratory helps me to apply what I have learnt to practice and offers me the chance to study further in the academic realm I interested in. I fell really lucky to be with the team which is one of those who take the lead in related domain.

First of all, I would like to express my deepest gratitude to my supervisor Prof. Yan, a venerable, responsible and amiable scholar, who has provided me with treasured guidance in every stage of my graduation project. Prof. Yan always exhorts me to treat scientific research with rigor. He said that our work to benefit patients is of great significance, our product would be applied to clinical medicine someday. No mistakes can be allowed. Even though graduation project does not ask high, respect to our work should still be showed and full efforts should still be devoted. His rigorous attitude towards academic and devotion to career like a day for decades has influenced profoundly on me.

I would also like to say thanks to my dear teachers, schoolmates, friends and all those who offered me a helping hand in the past days. It was them who taught me right from wrong. It was them who led me to step into the world of knowledge. It was them who patiently answered every single question from me. It was them who treated me with their warm heart like my family.

Then, I would like to thank my best family. Thanks for giving birth to me so that I can have the chance to feel the amazing world. Thanks for keeping me company, forgiving my unintentional blunders, sharing my happiness as well as anguish. Thanks for supporting me both materially and spiritually. You are the most cherished gift of my life.

What's more, I would like to express my deepest appreciation to my country and our party for the education I took, the safe and sound days and everything around.

Last but not least, thanks for reading!